DOI:
10.1016/j.taap.2008.06.006

Document Version
Peer reviewed version

Gene expression profiles modulated by the human carcinogen aristolochic acid I in human cancer cells and their dependence on *TP53*

Maria L. Simões[a], Sarah L. Hockley[a,†], Tanja Schwerdtle[b], Gonçalo Gamboa da Costa[a,‡], Heinz H. Schmeiser[c], David H. Phillips[a], Volker M. Arlt[a,*]

[a] *Section of Molecular Carcinogenesis, Institute of Cancer Research, Brookes Lawley Building, Cotswold Road, Sutton, Surrey SM2 5NG, United Kingdom*

[b] *Institute of Food Chemistry and Food Toxicology, Technical University of Berlin, TIB 4/3-1, Gustav-Meyer-Allee 25, D-13355 Berlin, Germany*

[c] *Division of Molecular Toxicology, German Cancer Research Center, Im Neuenheimer Feld 280, D-69120-Heidelberg, Germany*

*Corresponding author. Fax: +44 208 7224405. *E-mail address*: volker.arlt@icr.ac.uk.

[†] Present Address: Section of Haemato-Oncology, Institute of Cancer Research, Brookes Lawley Building, Cotswold Road, Sutton, Surrey SM2 5NG, United Kingdom

[‡] Present Address: Division of Biochemical Toxicology, National Center for Toxicological Research, Jefferson, AR 72079, USA

Abstract

Aristolochic acid (AA) is the causative agent of urothelial tumours associated with aristolochic acid nephropathy. These tumours contain *TP53* mutations and over-express TP53. We compared transcriptional and translational responses of two isogenic HCT116 cell lines, one expressing TP53 (p53-WT) and the other with this gene knocked out (p53-null), to treatment with aristolochic acid I (AAI) (50−100 μM) for 6–48 h. Modulation of 118 genes was observed in p53-WT cells and 123 genes in p53-null cells. Some genes, including *INSIG1*, *EGR1*, *CAV1*, *LCN2* and *CCNG1,* were differentially expressed in the two cell lines. *CDKN1A* was selectively up-regulated in p53-WT cells, leading to accumulation of TP53 and CDKN1A. Apoptotic signalling, measured by caspase-3 and -7 activity, was *TP53*-dependent. Both cell types accumulated in S phase, suggesting that AAI-DNA adducts interfere with DNA replication, independently of TP53 status. The oncogene *MYC*, frequently over-expressed in urothelial tumours, was up-regulated by AAI, whereas *FOS* was down-regulated. Observed modulation of genes involved in endocytosis, *e.g. RAB5A,* may be relevant to the known inhibition of receptor-mediated endocytosis, an early sign of AA-mediated proximal tubule injury. AAI-DNA adduct formation was significantly greater in p53-WT cells than in p53-null cells. Collectively, phenotypic anchoring of the AAI-induced expression profiles to DNA adduct formation, cell-cycle parameters, TP53 expression and apoptosis identified several genes linked to these biological outcomes, some of which are *TP53*-dependent. These results strengthen the importance of TP53 in AA-induced cancer, and indicate that other alterations, *e.g.* to MYC oncogenic pathways, may also contribute.

Keywords: Aristolochic acid, urothelial cancer, TP53, gene expression, apoptosis, microarray

Introduction

Aristolochic acid nephropathy (AAN) is a unique type of renal disease that predisposes patients to a high risk of urothelial cancer (Vanherweghem *et al.*, 1993; Nortier *et al.*, 2000; Lord *et al.*, 2001). The observed nephropathy has been traced to the ingestion of herbal medicinal remedies that have included *Aristolochia* species containing aristolochic acid (AA) (Arlt *et al.*, 2002). Natural health products containing AA are often sold as traditional Chinese medicines for weight loss, improving the immune system or alleviating gastrointestinal symptoms (Gold and Slone, 2003; Wu *et al.*, 2007). AA is a strong rodent carcinogen, being among the most potent 2% of known carcinogens (Gold and Slone, 2003). Herbal remedies containing *Aristolochia* species have been classified as carcinogenic to humans (Group 1) by the International Agency for Research on Cancer (IARC) (IARC, 2002).

AA is a mixture of two structurally similar nitro-phenanthrene carboxylic acids, aristolochic acid I (AAI) and aristolochic acid II (AAII). There is clear evidence that AA is a mutagen forming covalent DNA adducts (Arlt *et al.*, 2002). We have detected specific AA-DNA adducts in various tissues of AA-treated rats (Stiborova *et al.*, 1994) and in urothelial tissue of AAN patients (Schmeiser *et al.*, 1996; Nortier *et al.*, 2000). The most abundant DNA adduct detected was the adenosine adduct of AAI, 7-(deoxyadenosin-N^6-yl)aristolactam I (dA-AAI) (Schmeiser *et al.*, 1996; Nortier *et al.*, 2000; Lord *et al.*, 2001). Although AA-DNA adducts are also found in tissues outside the urinary tract (Arlt *et al.*, 2004), specific DNA damage due to AA in urothelial cells and cell-specific alterations of certain physiological processes (Lebeau *et al.*, 2001; Lebeau *et al.*, 2005) may explain the observed high incidence of urothelial tumours induced by AA.

The TP53 tumour suppressor functions as a key player in determining cell fate after DNA damage and disabling its function by mutations in its coding sequence leads to the development of tumours (Hussain *et al.*, 2000). More than 50% of all human tumours contain a *TP53* mutation (Petitjean *et al.*, 2007). Transcriptional modulation of *TP53*-target genes leads to the regulation of downstream processes, primarily cell-cycle arrest, apoptosis and DNA repair that protect the cell from DNA damage and transformation. AAN urothelial atypia have been associated with the over-expression of TP53, suggesting that *TP53* is mutated in AAN-associated tumours (Cosyns *et al.*, 1999; Arlt *et al.*, 2001b). Interestingly, in the one AAN patient available so far for analysis we found an AT→TA transversion mutation in *TP53* in urothelial tumour cells (Lord *et al.*, 2004). AT→TA transversions are typical mutations observed in the H-*ras* oncogene of tumours in rodents treated with AA and are consistent with AA-DNA adduct formation primarily at adenine residues (Schmeiser *et al.*, 1990; Arlt *et al.*, 2000). These data indicate a possible molecular mechanism whereby AA causes urothelial cancer.

Toxicogenomics can provide the means to define relationships between toxicological end-points and gene expression patterns, predict toxic responses, and identify mechanisms of toxicity of environmental agents such as AA (Chen *et al.*, 2006; Guo *et al.*, 2006; Stemmer *et al.*, 2007). In order to examine the role of TP53 in cellular responses to AA we have used cDNA microarrays to analyse transcriptional responses in a pair of human colorectal cell lines (HCT116) that differ in *TP53* status (*i.e.* wild-type [p53-WT] or knock-out [p53-null]) after exposure to the main component AAI and we have investigated the influence of duration of exposure and concentration of AAI on the observed responses. In addition, other biological parameters including DNA adduct formation, cell-cycle, apoptosis and protein expression were compared between the two cell lines.

Materials and Methods

Aristolochic acid I

A commercial natural plant extract AA (Roth, Germany) was subjected to three sequential recrystallizations from boiling dimethylformamide-water. The orange crystals thus dried under vacuum yielded around 98% pure AAI as determined by reversed-phase HPLC. The analysis of the AAI by high-field ^{1}H-NMR and mass spectrometry was fully consistent with its structure. AAI was converted to its sodium salt by neutralization with aqueous sodium hydroxide. The solution was thoroughly mixed and taken to dryness under reduced pressure, yielding the sodium salt of AAI quantitatively as a water-soluble deep-red amorphous powder.

Cell culture

Two isogenic HCT116 human colorectal carcinoma cell lines (Bunz *et al.*, 1998), one expressing wild-type *TP53* (p53-WT) and the other with complete knockout of *TP53* (p53-null), were kindly provided by B. Vogelstein, Johns Hopkins University School of Medicine, Baltimore, MD, USA. Cells were maintained in Dulbecco's modified Eagle's medium (DMEM) with Glutamax™ I, 1000 mg/L D-glucose and sodium pyruvate (Invitrogen, UK) and supplemented with 10% foetal bovine serum and 100 U penicillin/ml and 100 μg streptomycin/ml (Sigma Aldrich, UK). Cells were grown as adherent monolayers and sub-culturing was performed every 72 h when cells were 80% confluent and incubated in a humidified 5% CO_2 atmosphere at 37°C (Hockley *et al.*, 2008). For treatment, cells were grown for 48 h until 70% confluent and then the appropriate concentrations of AAI (as sodium salt) dissolved in water were added. Water only was added to control cultures. Cells were harvested by trypsinisation and then washed with PBS.

Cell viability and DNA adduct analysis

Cells (2.25×10^{6}) were seeded in T75 flasks in a total volume of 15 ml and after 48 h exposed to 0, 1, 10, 50 or 100 μM AAI. All incubations were performed in duplicate. Cell viability (% control) was determined using a Vi-Cell Cell Viability Analyzer (Beckman Coulter, UK) after exposure to AAI for 6, 24 or 48 h. Cells were spun down, and from each pellet DNA was isolated by a standard phenol chloroform extraction method (Arlt *et al.*, 2001b). DNA was quantified spectrophotometrically and DNA adducts were determined for each DNA sample (4 μg) using the nuclease P1 enrichment version of the ^{32}P-postlabelling method as described previously (Mei *et al.*, 2006; Phillips and Arlt, 2007). Chromatographic conditions for thin-layer chromatography (TLC) on polyethyleneimine-cellulose (PEI-cellulose) were: D1, 1.0 M sodium phosphate, pH 6.0; D3, 3.5

M lithium formate, 8.5 M urea, pH 4.0; and D4, 0.8 M lithium chloride, 0.5 M Tris-HCl, 8.5 M urea, pH 9.0. TLC sheets were scanned by using a Packard Instant Imager (Dowers Grove, IL, USA), and DNA adduct levels (RAL, relative adduct labelling) were calculated from the adduct cpm, the specific activity of [γ-^{32}P]ATP and the amount of DNA (pmol of DNA-P) used. Results were expressed as DNA adducts/10^8 nucleotides. Enzymatic preparations of AA-DNA adduct reference compounds were performed as described (Arlt *et al.*, 2001a). For DNA adduct formation, 3-Nitrobenzanthrone (3-NBA; 5 µM) was used as a positive control (Arlt *et al.*, 2005; Arlt *et al.*, 2007a).

Microarray and gene expression analysis

Cells (2.25×10^6) were seeded in T75 flasks in a total volume of 15 ml and after 48 h exposed to 0, 50 or 100 µM AAI. All incubations were performed in triplicate. After exposure to AAI for 6, 24 or 48 h cell pellets were collected and total RNA extracted using the Qiagen RNeasy Mini Kit protocol (RNeasy Mini Handbook, Qiagen, UK). After addition of lysis buffer (RLT, Qiagen) samples were homogenised using QIAshredders (Qiagen). RNA was quantified spectrophotometrically, and integrity was determined using a 2100 Bioanalyzer (Agilent Technologies, UK) so that only RNA samples that had an rRNA 28S/18S ratio greater than 1.5 were used for microarray analysis. Total RNA (4 µg) was reverse transcribed into cDNA and fluorescently labelled with Cy3 or Cy5 mono-reactive dyes (Amersham Biosciences, UK) using the Invitrogen Indirect cDNA Labelling Kit protocol (Invitrogen) as described (Hockley *et al.*, 2006; Hockley *et al.*, 2007; Hockley *et al.*, 2008).

Gene expression analysis was performed using the Cancer Research UK DNA Microarray Facility (CRUKDMF) Human 22K Genome-Wide Array v1.0.0. The full probe list for this array can be found at the CRUKDMF website (http://www.icr.ac.uk/array/array.html). The arrays were gridded onto Type 7* silanised slides (GE Healthcare, UK) followed and hybridisation, washing and scanning of the slides were performed as described (Hockley *et al.*, 2006; Hockley *et al.*, 2007). RNA from exposed cells and time-matched vehicle-treated control cells hybridised against each other for each dose and time-point from each triplicate biological experiment.

Image analysis using GenePix Pro v-5.1 software (Axon Instruments) and data normalisation within GeneSpring v-7.2 (Agilent Technologies, UK) were performed as described (Hockley *et al.*, 2008). Briefly, after Lowess normalisation and filtering out of unreliable data, triplicate biological replicates were averaged to identify genes with significantly ($P < 0.05$) altered expression by at least 1.4-fold. Log2 transformed data were used for any correlation (hierarchical clustering, principal components analysis [PCA]) and statistical algorithms (1-Way ANOVA)

performed within GeneSpring. The web-accessible program DAVID (Database for Annotation, Visualization, and Integrated Discovery) was used for functional gene annotation (Dennis *et al.*, 2003). Significant genes were uploaded into Expression Analysis Systematic Explorer (EASE version 2.0) for functional analysis (Hosack *et al.*, 2003). Biological processes significantly over-represented within the gene expression alterations had an EASE score assigned by EASE of less than 0.05.

The gene expression data discussed in this publication have been deposited in the National Center for Biotechnology (NCBI) Gene Expression Omnibus database (http://www.ncbi.nlm.nih.gov/geo/) and are accessible through GEO Series accession number GSE10359.

Real-time quantitative PCR (RTqPCR)

Two-step reverse transcription-PCR was used to generate cDNA for relative quantitation analysis using real-time fluorescent PCR on an ABI PRISM 7900HT Sequence Detection System (Applied Biosystems, UK) performed as previously described (Hockley *et al.*, 2006; Hockley *et al.*, 2007; Hockley *et al.*, 2008). To detect the modulated expression of selected target genes 20x Assays-On-Demand™ gene expression primers and probes (Applied Biosystems) were used (ALDH1A3-Hs00167476_m1, CCNG1-Hs00171112_m1, HIST1H4B-Hs00374342_s1, SCD-Hs00748952_s1, MYC-Hs00153408_m1, FOS-Hs00170630_m1, RHOB-Hs00269660_s1, NR1D1-Hs00253876_m1, CAV1-Hs00184697_m1, CDKN1A-Hs00355782_m1, and CYP1A1-Hs00153120_m1). Relative gene expression was calculated using the comparative threshold cycle (C_T) method.

Western blot analysis

For Western blot analysis 3×10^5 cells were seeded per well of a six-well plate in a total volume of 2 ml medium and exposed after 48 h to 0, 10, 50 or 100 μM AAI for 6, 24 or 48 h. Cell pellets were then collected and lysis and immunoblotting were performed as previously described (Hockley *et al.*, 2006; Hockley *et al.*, 2007; Hockley *et al.*, 2008). Monoclonal antibody against TP53 (Ab-6) was purchased from Calbiochem (Darmstadt, Germany) and diluted 1:5000. Detection of CDKN1A (p21) was by monoclonal antibody purchased from Santa Cruz Biotechnology (CA, USA), diluted 1:500. For detection of CYP1A1 we used a polyclonal antibody in a 1:500 dilution (Affinity BioReagents, Golden, CO, USA). Monoclonal antibody to detect GAPDH (6C5) was purchased

from Chemicon Europe (Hampshire, UK), diluted 1:5000 and used as a loading control. 3-NBA (5 μM) was used as a positive control.

Apoptosis assay

Cells were seeded (1.5×10^4 per well) in a 96-well plate in 0.1 ml medium and after 48 h exposed to 0, 50 or 100 μM AAI. All incubations were performed in triplicate. After exposure to AAI for 6, 24 or 48 h the activity of caspase-3 and -7 was measured using the Caspase-Glo assay kit (Promega, Southampton, UK) according to the manufacturer's instructions. Luminescent signal was detected using a Microtiter Plate Luminometer (DYNEX Technologies, UK). Luminescence was proportional to the amount of caspase activity present. 3-NBA (5 μM) was used as a positive control.

Flow cytometry

For cell cycle analysis 7.5×10^5 cells were seeded in T25 flasks in a total volume of 5 ml and after 48 h exposed to 0 or 100 μM AAI. All incubations were performed in duplicate. After exposure to AAI for 6, 24 or 48 h cells were fixed in ethanol as previously described (Hockley *et al.*, 2006). Fixed cells were stored at –20°C overnight, centrifuged (640 g, 3 min, 4°C) and after removing the supernatant 1 ml DAPI staining solution (Partec, Münster, Germany) was added. The samples were kept at room temperature for 4 h in the dark and analysed for DNA content using a PAS flow cytometer and FlowMax software (Partec, Münster, Germany) for evaluation of cell cycle distribution.

Induction of oxidative damage to DNA

DNA strand breaks and formamidopyrimidine-DNA glycosylase (Fpg)-sensitive sites were determined by the alkaline unwinding technique in combination with bacterial Fpg. Cells (7.5×10^5 cells) were seeded in T25 flasks in a total volume of 5 ml and after 48 h exposed to 0 or 100 μM AAI. All incubations were performed in duplicate. After exposure to AAI for 6, 24 or 48 h cells were prepared as described (Schwerdtle *et al.*, 2003). The Fpg protein was a generous gift of Dr. S. Boiteux (Commisariat Energie Atomique, Fontenay-aux-Roses, France) and used at a concentration of 1 μg/ml. For the detection of DNA strand breaks, Fpg was omitted. Unwinding of DNA, neutralisation and separation of single- and double-stranded DNA were performed as described previously (Hartwig *et al.*, 1996). The DNA content of both fractions was determined by adding Hochest 33258 and measuring the fluorescence with a spectrophotofluorometer (SPECTRA Fluor,

Tecan, Switzerland) at an excitation wavelength of 360 nm and an emission wavelength of 455 nm. The number of DNA strand breaks and Fpg-sensitive sites were calculated as described (Hartwig *et al.*, 1996). Hydrogen peroxide (H_2O_2; 100 μM for 5 min on ice) was used as a positive control.

Results

HCT116 p53-WT and p53-null cell viability

HCT116 p53-WT and p53-null cells were exposed to up to 100 μM AAI for up to 48 h to examine the effect of loss of TP53 function on cell viability (Figure 1). Short exposure time (6 h) and low AAI concentrations (1 or 10 μM) had little or no effect on cell viability in both cell lines. However, differences in viability between p53-WT and p53-null cells were observed after exposure to 50 or 100 μM AAI. A reduction in viable cells of up to 50% was observed in p53-WT cells after 24 and 48 h (Figure 1A). In p53-null cells no effect on cell viability was found after 24 h and at 50 μM, but exposure to 100 μM AAI resulted in up to a 30% reduction of viable cells at 48 h (Figure 1B).

DNA adduct analysis

DNA adduct formation in HCT116 p53-WT and p53-null cells exposed to up to 100 μM AAI (0, 10-100 μM) for up to 48 h was analysed using ^{32}P-postlabelling (Figure 2). In p53-WT cells the adduct pattern was qualitatively similar to that found in AAN patients, consisting of two major adduct spots (spots 1 and 2) and one minor (spot 3) (Schmeiser *et al.*, 1996; Bieler *et al.*, 1997; Nortier *et al.*, 2000). As shown in Figure 2A (inset), the two major adducts were identified as reported previously (Schmeiser *et al.*, 1996; Bieler *et al.*, 1997) as 7-(deoxyadenosin-N^6-yl)aristolactam I (spot 1; dA-AAI) and 7-deoxyguanosin-N^2-yl)aristolactam I (spot 2; dG-AAI), and the minor adduct as 7-(deoxyadenosin-N^6-yl)aristolactam II (spot 3; dA-AAII). In p53-null cells only exposure to 100 μM AAI for 48 h resulted in DNA adduct formation (Figure 2B; inset), dA-AAI being the only adduct detected. No DNA adducts were detected in controls (data not shown). Quantitative analysis obtained by ^{32}P-postlabelling revealed a dose-dependent formation of AA-DNA adducts in p53-WT cells (Figure 2A). Total AA-DNA adduct levels after 48 h ranged from 0.7 to 133 adducts per 10^8 nucleotides. In contrast, DNA adduct levels in p53-null cells were 3.5 adducts per 10^8 nucleotides (100 μM AAI; 48 h), being ~40-fold lower than those levels in p53-WT cells (Figure 2B). DNA adduct formation in p53-WT and p53-null cells was significantly different (P<0.05; Welch's two-sample t-test with adjustment for multiple corrections using Benjamin-Hocberg). Moreover, a multiple regression model fitted to the p53-WT DNA adduct data demonstrated a statistically significant linear trend for both time (P=0.031) and concentration (50 and 100 μM; P<0.0001). For 3-NBA, which was used as positive control, DNA adduct levels were similar in both pairs of cells (Figure 2).

Gene expression analysis

To determine differences in basal gene expression between the HCT116 p53-WT and p53-null cells, both cell lines were harvested 24 h after seeding and directly compared on the microarrays. GeneSpring software identified 32 (16 up-regulated, 16 down-regulated) cDNA clones that were significantly (P<0.05) modulated by at least 1.4-fold in p53-null relative to p53-WT cells (see Supporting Table 1 and 2). Genes up-regulated in the p53-null cells are likely candidates of transcriptional repression by functional TP53. Most notably, included in this list are 4 genes (*K-ALPHA-1*, *H2-ALPHA*, *TUBA-1* and *TUBA3*) that encode cytoskeletal proteins. This suggests that TP53 plays an important role in maintaining the expression of cell structural genes. The list of genes down-regulated in cells lacking TP53 confirms the genotypic status of these cells with transcripts of *TP53* and its transcriptional target *CDKN1A* significantly reduced relative to WT cells.

A principle aim of this study was to identify gene expression changes induced by AAI related to genotoxicity in relation to the *TP53* status at levels without severe cell toxicity. Therefore, AAI concentrations of 50 and 100 μM and exposure times of up to 48 h were chosen for the microarray experiments; these conditions resulted in DNA adduct formation, and induction of TP53 and CDKN1A proteins (see below; compare Figure 5) but not a severe reduction in cell viability. As shown in Figure 3A, filtering of Lowess normalised gene expression data at 50 and 100 μM at 6, 24 or 48 h in GeneSpring software identified 133 (82 up-regulated, 51 down-regulated) and 138 (67 up-regulated, 71 down-regulated) cDNA clones that were modulated by at least 1.4-fold and that had a significant t-test P value (<0.05) in at least one sample of the p53-WT and p53-null cells, respectively (see Supporting Tables 3 and 4). Sixty one genes were modulated in the same direction (39 up-regulated, 22 down-regulated) by AAI in both cell lines suggesting that these genes are modulated by *TP53*-independent mechanisms. AAI had very subtle effects on gene expression in both cell lines with few genes exceeding a 2-fold change in expression. Hierarchical clustering of the gene expression profiles revealed that the gene expression profiles were relatively similar after exposure to 50 μM AAI and an exposure period of 6 h, independently of *TP53* status (Figure 4A). However, gene expression profiles at 100 μM AAI clustered according to longer exposure times (24 and 48 h) and *TP53* status. PCA confirmed that, overall, AAI-induced gene expression profiles were more dependent on the concentration tested and the longer exposure time, than on the *TP53* status of the cells (Figure 4B). Thus, for functional gene expression analysis we focused only on gene changes observed at 100 μM AAI for 24 and 48 h.

As shown in Figure 3B, 118 genes in total (77 up-regulated, 41 down-regulated) were significantly modulated by at least 1.4-fold in p53-WT and 123 genes (58 up-regulated, 65 down-

regulated) in p53-null cells (see Supporting Tables 5 and 6), confirming that most of the gene changes found occurred only at the highest concentration tested (100 μM) and after longer exposure times (24 and 48 h; compare Figure 3A). The program DAVID (Dennis *et al.*, 2003) was used for functional gene annotation. The most up-regulated genes in p53-WT cells were *KLF10* and *EGR1*. The early growth response 1 (*EGR1*) gene is a transcription factor that acts both as a tumour suppressor and as a tumour promoter (Krones-Herzig *et al.*, 2005). In p53-null cells *NR1D1* was the most up-regulated gene, which is linked to the mammalian circadian rhythm (Preitner *et al.*, 2002). *SCD* which encodes for stearoyl-CoA desaturase involved in fatty acid biosynthesis was the most down-regulated gene in both cell lines. We found that a number of histone genes (*HIST1H1C*, *HIST1H2AC*, *HIST1H3D*, *HIST1H3E*, *HIST1H4B*, and *HIST1H4C*) were strongly up-regulated both in p53-WT and p53-null cells. We also found gene expression changes in oncogenes, such as *MYC* and *RHOB*, which were both up-regulated only in p53-null cells, and *FOS*, which was down-regulated in both cell lines. Two changed genes were associated with endocytosis (*NECAP1* and *RAB5A*) which may be important as AA was previously shown to inhibit receptor-mediated endocytosis (Lebeau *et al.*, 2001; Lebeau *et al.*, 2005). A number of gene changes in p53-WT (*CDKN1A*, *CSE1L*, *CTNNAL1*, *NFKBIA*, *PPP2CA*, *STRN3*, and *UBE2V2*) and p53-null cells (*MYC*, *CCNG1*, *RPA2*, and *YARS*) were linked with apoptosis and/or cell cycle regulation. One gene, *XRCC4*, was linked to DNA repair and was up-regulated only in p53-WT cells.

An overlap of 56 genes (37 up-regulated, 19 down-regulated) was found in p53-WT and p53-null cells after AAI exposure suggesting that these genes are modulated independently from *TP53*. In GeneSpring, 1-Way ANOVA was performed on the list of all genes modulated by AAI in the two cell lines (185 genes) to identify genes that are the most differently expressed between p53-WT and p53-null cells. These *TP53*-discriminating genes with their associated expression ratios can be seen in Table 1. *EGR1*, *INSIG1* and *NR1D1* are involved in regulation of transcription; *CAV1*, *CCNG1*, *INSIG1*, *LCN2* and *PLP2* are involved in cell growth and/or maintenance. Encouragingly, this list includes *TP53*-regulated genes such as *CCNG1* which is involved in cell cycle regulation (Ohtsuka *et al.*, 2004). *CCNG1* and *CAV1* were down-regulated only in p53-null cells. Although *EGR1* was up-regulated in both cell lines, it was up-regulated much more strongly in p53-WT cells. Two genes that are involved in metabolism, *CPM* and *ALDH1A3*, were up-regulated only in p53-WT cells.

To determine whether any biological themes exist within the expression data of the HCT116 cells exposed to AAI, EASE analysis was performed to identify biological processes that are significantly over-represented (EASE score <0.05) in the gene lists when compared to their total representation on the microarray (Table 2). Over-represented themes among the up-regulated genes

in both cell lines included regulation of transcription (*e.g.* RNA splicing/processing/metabolism), replication (*e.g.* nucleic acid metabolism and chromatin assembly/disassembly) and metabolism (*e.g.* amino acid and carbohydrate metabolism, protein biosynthesis). No over-represented themes were found among the down-regulated genes in p53-WT cells. In p53-null cells this list included biosynthesis (e.g. protein and macromolecule biosynthesis), metabolism (*e.g.* protein metabolism) and secretion.

RTqPCR

RTqPCR, a more sensitive and specific measure of gene expression, was carried out in HCT116 p53-WT and p53-null cells exposed to 0 or 100 μM AAI for 48 h to validate a number of interesting expression changes and to validate the microarray data. Ten genes (*ALDH1A3*, *CCNG1*, *HIST1H4B*, *SCD*, *MYC*, *FOS*, *ROHB*, *NR1D1*, *CAV1*, and *CDKN1A*) were selected to be measured by RTqPCR. In the majority of cases the RTqPCR data confirmed the microarray data (Table 3). Agreement between the microarray and RTqPCR was 80% which is consistent with a previous study using the same microarray (Hockley *et al.*, 2007). *CDKN1A* was strongly up-regulated in p53-WT cells using RTqPCR confirming results obtained on the protein level (see below; compare Figure 5B). Although *MYC* was up-regulated significantly on the microarray in p53-WT cells, its modulation was slightly below the cut-off of 1.4 (data not shown). However, using RTqPCR *MYC* was clearly overexpressed in p53-WT cells after AAI exposure, indicating that RTqPCR is a more sensitive measure of gene expression in this case. RTqPCR was also used to measure the expression of *CYP1A1*, known to be involved in the metabolic activation of AA (Stiborova *et al.*, 2005; Stiborova *et al.*, 2008), but not present on the microarray. Increased expression of *CYP1A1*was found in both cell lines, although the expression level was lower in the p53-null cells (Table 3).

Western blot analysis

TP53 levels in HCT116 p53-WT and p53-null cells were assessed by Western blot analysis in order to confirm its accumulation in response to the AAI concentrations used. Protein levels were analysed in both cell lines exposed to up to 100 μM AAI (0, 10-100 μM) for up to 48 h (Figure 5). As expected, TP53 was not detectable in p53-null cells (Figure 5A). In p53-WT cells no increase in TP53 in comparison to controls was observed after 6 (data not shown) and 24 h; induction of TP53 was observed only after exposure to 50 or 100 μM AAI for 48 h. A similar expression pattern was found for CDKN1A accumulation (Figure 5B). Clear CDKN1A induction was observed in p53-WT cells, but only after exposure to 50 or 100 μM AAI for 48 h. Basal levels of CDKN1A observed in

p53-null cells at 48 h remained unchanged by AAI-treatment. For 3-NBA, which was used as positive control, induction of TP53 and CDKN1A was observed in p53-WT cells only (data not shown). Since AAI is known to be metabolically activated by CYP1A1 (Stiborova *et al.*, 2005; Stiborova *et al.*, 2008), we investigated CYP1A1 expression in both cell lines. No difference in the basal or induction levels of CYP1A1 between p53-WT and p53-null cells was observed (data not shown).

Apoptosis measurement

To examine apoptotic signalling in HCT116 p53-WT and p53-null cells after AAI exposure, the activities of two key effector enzymes that are involved in apoptosis in mammalian cells, caspase-3 and -7, were measured by luminescence detection. While there was no difference in caspase activity observed in p53-null cells, increased activity was found in p53-WT cells after 24 and 48 h at 100 μM AAI (Figure 6). Using a linear model with caspase activity being the response variable and explanatory variables TP53 status (categorical) and time (continuous) we found a statistically significant increase in caspase activity with time in p53-WT cells ($P<0.0001$). The time-dependent response was significantly different in p53-WT and p53-null cells ($P<0.0001$). This is consistent with the cell viability and DNA adduct data where the greatest loss of viability and DNA adduct formation only occurred in p53-WT cells. 3-NBA (5 μM), used as positive control, strongly induced caspase activity in a time-dependent manner, independent of the *TP53* status (Figure 6). The latter observation is consistent with the finding that 3-NBA induces equally high levels of DNA adducts in both HCT116 p53-WT and p53-null cells (Hockley *et al.*, 2008).

Flow cytometry

The identification of altered expression of transcripts that may affect cell cycle regulation and genes whose expression is tightly coupled with DNA metabolism, prompted the investigation of the effects of AAI on the cell cycle parameters in HCT116 p53-WT and p53-null cells. The DNA content of cells exposed to 0 or 100 μM AAI for up to 48 h was measured by FACS analysis (Figure 7). There was a clear accumulation of both cell types in the S phase after 24 and 48 h exposure to AAI when compared to controls ($P<0.0001$; Welch's two-sample *t*-test using Benjamin Hocberg multiple testing correction). Arrest in the S phase implies that DNA synthesis is being inhibited in both cell types in response to AAI exposure. The fold increase in cells in S phase was similar in both cell lines indicating that the alterations of the cell cycle parameters do not depend on *TP53* ($P=0.274$; ANOVA).

Induction of DNA strand breaks and oxidative DNA base modifications

To assess the induction of DNA strand breaks and oxidative DNA base modifications by AAI, HCT116 cells were exposed to 0 or 100 μM AAI for up to 48 h and lesion frequencies were quantified by the alkaline unwinding technique in combination with the bacterial Fpg (Hartwig *et al.*, 1996). Fpg recognises 7,8-dihydro-8-oxoguanine (8-oxoguanine), 2,6-diamino-4-hydroxy-5-formamindopyrimidine (Fapy-Gua), 4,6-diamino-5-formamido-pyrimidine (Fapy-Ade) and to a smaller extent 7,8-dihydro-8-oxoadenine (8-oxoadenine) as well as apurinic/apyrimidinic sites (AP sites) and converts them into DNA strand breaks by its associated DNA endonuclease activity (Tchou *et al.*, 1991; Boiteux *et al.*, 1992). In untreated p53-WT and p53-null cells similar amounts of double stranded DNA in the absence and presence of Fpg were measured, demonstrating comparable background levels of DNA strand breaks and Fpg-sensitive sites. Overall, as shown in Figure 8, for all incubation times we observed only low level of DNA strand breaks, up to 0.2 lesions/10^6 base pairs in both p53-WT and p53-null cells. A 5-min incubation of both pairs of cells with 100 μM hydrogen peroxide on ice (to omit DNA repair) as a positive control induced similar levels of DNA strand breaks and Fpg-sensitive sites, being up to 10-fold higher compared with cells treated with AAI (Figure 8). Although only low levels of DNA strand breaks were detected following exposure to AAI for 48 h, around twice as many DNA strand breaks were found in p53-WT relative to p53-null cells. Similarly, only low levels of Fpg-sensitive sites were observed in both p53-WT and p53-null cells (Figure 8). Despite these low levels, after 48 h exposure to AAI around 2-times more Fpg-sensitive sites were detected in p53-null relative to p53-WT cells. It is noteworthy that TP53 has been assumed to be the major regulator of the expression and activity of the human 8-oxoguanine-DNA glycosylase (hOgg1) (Chatterjee *et al.*, 2006), suggesting that in p53-null cells Fpg-sensitive sites are repaired much more slowly due to reduced expression levels of Ogg1, resulting in the higher accumulation of Fpg-sensitive sites in p53-null relative to p53-WT cells.

Discussion

TP53 plays a key role in cellular response to genotoxic stress and is involved in several critical pathways including cell-cycle arrest, apoptosis, DNA repair and cellular senescence, which are essential to maintain genome integrity (Hussain *et al.*, 2000). The importance of this protein is highlighted by the fact that it is mutated in 50% of human tumours (Petitjean *et al.*, 2007). Using microarray technology AA-characteristic gene expression profiles were observed recently in rodents receiving short-term treatment with AA providing novel information on molecular mechanisms underlying AA-induced carcinogenesis (Chen *et al.*, 2006; Stemmer *et al.*, 2007). To investigate the role of TP53 in the cellular response to AA we compared the transcriptional and translational responses to AAI in human cells that differ in *TP53* status. While no urothelial cell lines with disrupted *TP53* were available, colorectal HCT116 cells with wild-type (p53-WT) or homozygously disrupted *TP53* (p53-null) (Bunz *et al.*, 1998) have been proven to be a valuable tool to examine gene expression profiles associated with the TP53 network in response to cellular stress and environmental carcinogens (Staib *et al.*, 2005; Hockley *et al.*, 2008). Moreover, in various genotoxicity studies HCT116 cells were found to metabolically activate a variety of different genotoxic agents (McDermott *et al.*, 2005; Arlt *et al.*, 2007a; Dornetshuber *et al.*, 2007; Hockley *et al.*, 2008). Among the compounds activated were nitro polycyclic aromatic hydrocarbons, demonstrating that these cells can catalyse bioactivation by nitroreduction (Arlt *et al.*, 2007a), which is the major activation pathway for AA (Arlt *et al.*, 2002; Stiborova *et al.*, 2005; Stiborova *et al.*, 2008).

AAN urothelial atypia have been associated with the overexpression of TP53 (Cosyns *et al.*, 1999), indicating its cellular accumulation in response to AA-induced DNA damage. Mutated TP53 is often over-expressed in tumour cells and increasing evidence suggests that mutant *TP53* is not only responsible for the loss of the tumour-suppressive functions but may also result in additional pro-oncogenic properties (Vikhanskaya *et al.*, 2007). In the present study we found TP53 accumulation in HCT116 p53-WT cells after AAI exposure. Interestingly, DNA adduct analysis revealed that adduct levels were ~40-fold higher in p53-WT cells at a dose (100 μM) and time point (48 h) where AA-DNA adducts were detected in both cell lines. DNA adduct levels induced by AAI in p53-WT cells was comparable to those observed in human breast carcinoma MCF-7 cells exposed to similar concentrations of AAI (10-100 μM) (Arlt *et al.*, 2001b). AAI-DNA adducts have been linked with specific AT→TA transversion mutations in codon 61 of the *H*-ras gene leading to activation of this oncogene in AAI-induced tumours in rodents (Schmeiser *et al.*, 1990; Arlt *et al.*, 2000). The same type of mutation was found in *TP53* in urothelial tumour cells of an AAN patient

(Lord *et al.*, 2004), suggesting that *TP53* is mutated in AAN-associated tumours (Arlt *et al.*, 2001b; Arlt *et al.*, 2007b). Furthermore, AT→TA transversions were found in *TP53* of immortalised cells derived from murine primary human *TP53* knock-in (Hupki) embryonic fibroblasts exposed to AAI (Liu *et al.*, 2004; Feldmeyer *et al.*, 2006; vom Brocke *et al.*, 2006). Interestingly, in one cell line the mutation was in codon 139, identical to one found in the urothelial tumour cells of the AAN patient (Lord *et al.*, 2004; Feldmeyer *et al.*, 2006). Moreover, a high frequency of AT→TA transversion mutations was found in the *TP53* of urothelial tumours from patients with Balkan endemic nephropathy and exposed to AA (Grollman *et al.*, 2007). These data indicate that TP53 plays an important role in the molecular mechanism whereby AA causes urothelial cancer (Arlt *et al.*, 2007b). In HCT116 cells exposed to benzo(a)pyrene (BaP) DNA adduct formation was also dependent on *TP53*, being significantly lower in p53-null than in p53-WT cells (Hockley *et al.*, 2008), suggesting that basal levels of TP53 are linked to the metabolic activation of both BaP and AAI. In contrast, no influence of *TP53* on DNA adduct formation was seen after treatment of p53-WT and p53-null cells with the diol-epoxide of BaP (BPDE) or with 3-NBA (Hockley *et al.*, 2008). As the mechanism for the influence of *TP53* on xenobiotic metabolism is not yet understood, the TP53-dependent effect on AA-DNA adduct formation requires further investigation.

Using cDNA microrray and RTqPCR we found only subtle changes in gene expression in p53-WT and p53-null cells after exposure to AAI and transcriptional responses were only evident at higher concentrations and after a longer duration of exposure. This was reflected in cell viability and may be due to the levels of DNA damage not being high enough to elicit a greater response. A small sub-set of gene expression changes were identified as discriminating *TP53* status in AAI-treated HCT116 cells but the *TP53* status of the cells was only apparently critical after a longer exposure time of 24 h and at the highest concentration tested (100 μM). This may be the result of downstream gene expression alterations, dependent on TP53 activation, coming into effect over time. Similarly, BPDE induced a small number of *TP53*-dependent gene expression changes in these cells, although the number of *TP53*-regulated genes was greater than in the present study (Hockley *et al.*, 2008). In Eker and WT rats treated with 10 mg/kg bw of AA (41% AAI, 56% AAII) for up to 14 days the *TP53*-regulated genes *CDKN1A* and *CCNG1* were changed (up-regulated) in a time-dependent manner (Stemmer *et al.*, 2007). We found that *CDKN1A* and *CCNG1* were changed in HCT116 cells exposed to AAI and these genes were identified as discriminating *TP53* status in TK6 cells after DNA-damaging treatments (Amundson *et al.*, 2005). *CDKN1A* encodes a potent cell cycle inhibitor, regulating cell cycle progression at the G1 and G2 check-points in response to a variety of stress stimuli (el-Deiry *et al.*, 1994; Ohtsuka *et al.*, 2004), and was strongly up-regulated in p53-WT cells after AAI exposure (see below). Genes identified as

discriminating *TP53* status in HCT116 cells after AAI exposure included *CCNG1*, *EGR1*, *CAV1*, *NR1D1*, and *LCN2*. *CCNG1* encodes cyclin G1, which has growth inhibitory activity (Ohtsuka *et al.*, 2004) and was strongly down-regulated in AAI-treated p53-null cells. It has been suggested that cyclin G-mediated TP53 regulation is dependent upon the status of ataxia-telangiectasia mutated (ATM) protein, which activates TP53 in response to DNA damage (Ohtsuka *et al.*, 2004). The transcription factor early growth response 1 (*EGR1*) gene, which was one of the most highly up-regulated genes in p53-WT cells, is a direct regulator of multiple tumour suppressors including TGFβ1, PTEN, TP53 and fibronectin (Krones-Herzig *et al.*, 2005; Baron *et al.*, 2006). EGR1 has important tumour suppressor properties, *e.g.* via the direct induction of the epithelial cell suppressor TGFβ1 and the direct induction of TP53 to promote apoptosis. *CAV1* encodes for caveolin-1 that has been linked with oncogenic transformation, cancer and metastasis (Carver and Schnitzer, 2003; Williams and Lisanti, 2005) and was down-regulated in p53-null cells along with *CAV2*. *NR1D1* encodes for the orphan nuclear receptor Rev-Erbα, which is the major regulator of cyclic *Bmal1* transcription as part of the mammalian circadian rhythm (Preitner *et al.*, 2002). Besides *NR1D1*, *NR1D2* was also up-regulated both in p53-WT and p53-null cells. It is thought that disruption of the circadian rhythm may increase cancer risk (Gauger and Sancar, 2005). *LCN2*, which encodes for lipocalin 2, plays a role in cell regulation and penetration of lipophilic ligands through the cell membrane after lipocalin-mediated transport to the cell surface and interaction with cytosolic and/or nuclear proteins (see below) (Bratt, 2000; Hvidberg *et al.*, 2005). Lipocalins have been linked with cancer development (Bratt, 2000). Although the list of *TP53*-dependent identified signature genes is small, this observation is consistent with other studies (Park *et al.*, 2002; Amundson *et al.*, 2005; Hockley *et al.*, 2008). Therefore, the present study also shows that expression profiles induced by AAI are largely *TP53*-independent in HCT116 cells. However, we found AAI-induced apoptosis in HCT116 p53-WT cells but not in p53-null cells, indicating that apoptotic signalling, as measured by caspase activity, is *TP53*-dependent.

Tubular atrophy is a pathohistological feature in AAN (Cosyns, 2003) and AA-induced apoptosis in tubular cells may be responsible for it (Pozdzik *et al.*, 2008). Indeed, apoptotic cells were detected *in vivo* within renal tubules of AA-treated rodents (Okada *et al.*, 2003; Pozdzik *et al.*, 2008). Others have demonstrated that AA induces apoptosis *in vitro* in renal tubular cells (Balachandran *et al.*, 2005; Hsin *et al.*, 2006; Li *et al.*, 2006; Qi *et al.*, 2007). In porcine proximale tubular epithelial LLC-PK1 cells AA-induced apoptosis was associated with an increase in intracellular calcium concentration (Li *et al.*, 2006). In canine renal distal tubular MDCK and human tubular epithelial HK-2 cells AA/AAI had an impact on the Ca^{2+} homeostasis by activating

Ca^{2+}-release channels and/or inhibiting Ca^{2+}-ATPases, causing both endoplasmic reticulum and mitochondria stress (Hsin *et al.*, 2006; Qi *et al.*, 2007). Interestingly, *INSIG1* was down-regulated in HCT116 p53-WT cells after AAI exposure, INSIG1 being a protein closely related to endoplasmic reticulum proteins inducing cellular stress through its depletion (Lee and Ye, 2004). Moreover, *CAPNS1* was down-regulated in both HCT116 p53-WT and p53-null cells after AAI exposure. Calpains are a family of Ca^{2+}-dependent neutral cysteine proteases involved in a number of cellular events including apoptosis (Del Bello *et al.*, 2007; Pineiro *et al.*, 2007). Although the role of calpains in apoptosis is still poorly understood, results show a promoting or a protective role depending on the cell type studied, depending particularly on the concomitant involvement of the caspase machinery (Neumar *et al.*, 2003). It is possible that the impact of AA exposure on the intracellular Ca^{2+} concentration (Hsin *et al.*, 2006; Qi *et al.*, 2007) may be linked to a modulation of calpain activity, and that calpain subsequently produces proteolysis of caspase-3 (as measured in the present study), thereby triggering apoptosis. Indeed caspase-3 and -7 activity was also increased in LLC-PK1 and HK-2 cells treated with AAI (Balachandran *et al.*, 2005; Qi *et al.*, 2007). Calpain acts upstream of TP53, and it was shown that calpain inhibition up-regulates TP53 levels and induces apoptosis in human tumour cell lines (Atencio *et al.*, 2000). This could explain the *TP53*-dependence of apoptosis in HCT116 cells as it only occurred in p53-WT cells. However, the role of calpains in AA-induced apoptosis requires further investigation.

A number of DNA-damaging agents have been shown to activate TP53 and inhibit cell growth by arrest at the G1/S boundary of the cell cycle (Dipple *et al.*, 1999; Khan *et al.*, 1999). This cell cycle arrest is thought to be an important cellular defence mechanism that prevents replication of damaged DNA. This arrest in G1 phase is mediated by TP53, which is stabilized as a result of DNA damage (el-Deiry *et al.*, 1994). We found that exposure to AAI caused an accumulation of both p53-WT and p53-null cells in S phase. We showed that AAI selectively slows down the progression of HCT116 cells through S phase. Transcriptional activation of histone genes has been found in cells at the G1/S transition and during S phase (Stein *et al.*, 2006). In the present study we observed up-regulation of *HIST1H1C*, *HIST1H2AC*, *HIST1H3D*, *HIST1H3E*, *HIST1H4B* and *HIST1H4C* in HCT116 cells exposed to AAI, indicating a transcriptional activation of these genes in response to accumulation of cells in S phase. It is tempting to speculate that the mechanism of the S phase delay is the inability of the DNA polymerase complex to replicate over AAI-induced DNA adducts. It has been shown that DNA damage blocks DNA replication and/or transcription by polymerase (Roos and Kaina, 2006). Indeed this has been observed in AA-modified DNA templates, demonstrating that AA-DNA adducts can efficiently block DNA polymerase (Broschard *et al.*, 1994; Arlt *et al.*, 2000; Arlt *et al.*, 2001b). Inhibition of DNA replication has also been implicated

as a proximate initiator of apoptosis (Roos and Kaina, 2006), which we found in p53-WT cells (see above). However, since AAI-mediated S phase arrest was seen in both p53-WT and p53-null cells, this indicates that its mechanism is *TP53*-independent. The concept of a stealth property of cells to evade a protective G1 arrest after DNA damage has been described for other potent carcinogens (*e.g.* polycyclic aromatic hydrocarbons and aflatoxin) (Khan *et al.*, 1997; Khan and Dipple, 2000; Ricordy *et al.*, 2002). Similarly, treatment of HCT116 p53-WT and p53-null cells with BPDE resulted in accumulation of cells in S phase and was independent of the cells' *TP53* status (Hockley *et al.*, 2008), which is consistent with our findings. It has been suggested that lack of G1 arrest is through the inability of cells to induce the expression of the potent G1/G2 cell cycle inhibitor, CDKN1A (Khan *et al.*, 1997). In this study, we saw accumulation of CDKN1A in p53-WT cells after AAI exposure for 48 h, but not for 24 h, a time-point at which S-phase accumulation already occurred. Similarly, only at the latest time-point (48 h) was TP53 accumulation observed in p53-WT cells. In HCT116 p53-WT cells exposed to BPDE, accumulation of CDKN1A was found at time-points at which accumulation of cells in S phase was observed, but no G1 arrest occurred (Hockley *et al.*, 2008). In contrast, a dose-dependent G1 arrest was found in human urinary tract epithelium SV-HUC-1 cells following treatment with AA (41% AAI, 56% AAII) at a similar concentration to that used in our study (100 μM) (Chang *et al.*, 2007). Consistent with this functional outcome, levels of TP53 and CDKN1A were increased in AA-treated SV-HUC-1 cells. Moreover a decrease in the activity of cyclin E/cdk2 complex was induced by the increase of TP53 and CDKN1A, resulting in pRB hypophosphorylation, preventing AA-treated SV-HUC-1 cells undergoing transition to S phase (Chang *et al.*, 2007). Although TP53 and CDKN1A accumulation (at 24 h) and cell cycle parameters (at 48 h) in SV-HUC-1 cells have been measured only at different time-points (Chang *et al.*, 2007), the strong induction of TP53 and CDKN1A seen after 24 h may suggest that higher initial DNA damage (AA-DNA adduct level) is probably responsible for the observed G1 arrest after 48 h. Besides cell-type specific effects, it is tempting to speculate that the lower AAI-induced DNA adduct levels in HCT116 p53-WT and p53-null cells after 24 h account for a difference in the rate of TP53 accumulation and induction of CDKN1A. Subsequently, levels of the latter proteins were not high enough to trigger G1 arrest. Consequently, replication of AA-damaged DNA may result in mutation leading to malignant transformation of the AA-exposed cells (Khan and Dipple, 2000).

Previous studies have indicated that a subset of urothelial cancers might have a strong predisposition to gene amplification, and that crucial genetic alterations other than *TP53* mutations might be responsible for this predisposition (Schulz, 2006). For example, MYC overexpression has been found frequently in advanced urothelial carcinomas (Habuchi *et al.*, 1994; Grimm *et al.*, 1995;

Schulz *et al.*, 1998), and this may also have some relevance in AAN-associated urothelial carcinomas, although this has not yet been investigated in clinical samples. Interestingly, we found up-regulation of *MYC* in HCT116 cells after AAI exposure, although this was not clearly apparent at the protein level. MYC is required in normal cells for cell cycle competence, whereas in tumour cells it is over-expressed and functions as the angiogenic switch (Nilsson and Cleveland, 2003). Other oncogenes with altered expression in AAI-treated HCT116 cells included *FOS* (down-regulated) and *ROHB* (up-regulated), both genes linked to progression of human cancers (Kamai *et al.*, 2003; Wheeler and Ridley, 2004; Milde-Langosch, 2005). *RAS* is another oncogene that has been shown to be activated (mutated) in AA-induced tumours (Schmeiser *et al.*, 1990). Thus, in addition to *TP53*, disruption of oncogenic pathways of *e.g. MYC*, *RAS*, *FOS* and/or *ROHB* may be involved in the development and progression of AA-induced urothelial tumours, and may be valuable prognostic markers in future clinical studies.

One of the earliest clinical signs of AAN is urinary excretion of low-molecular-weight proteins, indicating that AA is toxic to proximal tubule cells (Kabanda *et al.*, 1995). Indeed, previous studies have shown that AA inhibits receptor-mediated endocytosis of low-molecular-weight proteins in proximal tubule cells, which is associated with decreased megalin expression (Lebeau *et al.*, 2001; Lebeau *et al.*, 2005). It is noteworthy that the endocytotic receptor megalin binds the transporting neutrophil-gelatinase-associated lipocalin (LCN2) with high affinity and mediates its cellular uptake (Hvidberg *et al.*, 2005). *LCN2* was selectively down-regulated in HCT116 p53-WT cells after AAI exposure. In opossum kidney cells a causal relationship between AA-DNA adduct formation and the inhibition of receptor-mediated endocytosis was found, suggesting that AA-DNA adducts might impair such physiological processes (Lebeau *et al.*, 2001). Interestingly, we found two genes linked to endocytosis in HCT116 cells exposed to AAI, namely *NECAP1* (down-regulated) and *RAB5A* (up-regulated). NECAP1 has been shown to play a role in clathrin-mediated endocytosis, although its precise function is unclear (Ritter *et al.*, 2003). A function of RAB5A is to regulate endosome fusion, but a key role for this small GTPase in the initial phases of receptor-mediated endocytosis is also emerging (Lanzetti *et al.*, 2001; Christensen *et al.*, 2003). Thus, changes in *NECAP1* and *RAB5A* expression may play a role in AA-induced inhibition of receptor-mediated endocytosis.

Conclusions

Phenotypic anchoring of the AAI-induced expression profiles to DNA adduct formation, cell cycle parameters, TP53 protein expression and apoptosis identified a number of genes that are linked to these biological outcomes. Some of them are *TP53*-dependent, thereby indicating them as target

genes in the development of AA-induced carcinogenesis. Although these results strengthen the important role of TP53 in AA-induced cancer, crucial genetic alterations other than *TP53* mutations (*e.g.* disruption of oncogenic pathways such as *MYC*) may also contribute to tumour development.

Acknowledgements

We thank the Cancer Research UK DNA Microarray Facility for the production of the microarrays and Drs. Ian Giddings and Daniel Brewer for advice and help with the statistical analysis. This work was supported by the Association for International Cancer Research (AICR) and Cancer Research UK. SLH received a PhD studendship from the Institute of Cancer Research. Work in the laboratory of TS is supported by the German Research Foundation (DFG). MLS, SLH, GGC, DHP and VMA are members of ECNIS (Environmental Cancer Risk, Nutrition and Individual Susceptibility), a Network of Excellence operating with the European Union 6th Framework Program, Priority 5: "Food Quality and Safety" (Contract No. 513943).

Supporting Information Available:

Supporting Table 1: full list of genes significantly (P<0.05) up-regulated by at least 1.4-fold in HCT116 p53-null relative to p53-WT cells; Supporting Table 2: full list of genes significantly (P<0.05) down-regulated by at least 1.4-fold in HCT116 p53-null relative to p53-WT cells; Supporting Table 3: full list of genes identified as significantly (P<0.05) modulated by at least 1.4-fold in HCT116 p53-WT cells after exposure to AAI; Supporting Table 4: full list of genes identified as significantly (P<0.05) modulated by at least 1.4-fold in HCT116 p53-null cells after exposure to AAI; Supporting Table 5: full list of genes identified as significantly (P<0.05) modulated by at least 1.4-fold in HCT116 p53-WT cells after exposure to 100 μM AAI for 24 or 48 hours; Supporting Table 6: full list of genes identified as significantly (P<0.05) modulated by at least 1.4-fold in HCT116 p53-null cells after exposure to 100 μM AAI for 24 or 48 hours.

References

Amundson, S.A., Do, K.T., Vinikoor, L., Koch-Paiz, C.A., Bittner, M.L., Trent, J.M., Meltzer, P., Fornace, A.J., Jr., 2005. Stress-specific signatures: expression profiling of p53 wild-type and -null human cells. Oncogene 24, 4572-4579.

Arlt, V.M., Wiessler, M., Schmeiser, H.H., 2000. Using polymerase arrest to detect DNA binding specificity of aristolochic acid in the mouse H-ras gene. Carcinogenesis 21, 235-242.

Arlt, V.M., Pfohl-Leszkowicz, A., Cosyns, J., Schmeiser, H.H., 2001a. Analyses of DNA adducts formed by ochratoxin A and aristolochic acid in patients with Chinese herbs nephropathy. Mutat. Res. 494, 143-150.

Arlt, V.M., Schmeiser, H.H., Pfeifer, G.P., 2001b. Sequence-specific detection of aristolochic acid-DNA adducts in the human p53 gene by terminal transferase-dependent PCR. Carcinogenesis 22, 133-140.

Arlt, V.M., Stiborova, M., Schmeiser, H.H., 2002. Aristolochic acid as a probable human cancer hazard in herbal remedies: a review. Mutagenesis 17, 265-277.

Arlt, V.M., Alunni-Perret, V., Quatrehomme, G., Ohayon, P., Albano, L., Gaid, H., Michiels, J.F., Meyrier, A., Cassuto, E., Wiessler, M., Schmeiser, H.H., Cosyns, J.P., 2004. Aristolochic acid (AA)-DNA adduct as marker of AA exposure and risk factor for AA nephropathy-associated cancer. Int. J. Cancer 111, 977-980.

Arlt, V.M., Stiborova, M., Henderson, C.J., Osborne, M.R., Bieler, C.A., Frei, E., Martinek, V., Sopko, B., Wolf, C.R., Schmeiser, H.H., Phillips, D.H., 2005. Environmental pollutant and potent mutagen 3-nitrobenzanthrone forms DNA adducts after reduction by NAD(P)H:quinone oxidoreductase and conjugation by acetyltransferases and sulfotransferases in human hepatic cytosols. Cancer Res. 65, 2644-2652.

Arlt, V.M., Glatt, H., Gamboa da Costa, G., Reynisson, J., Takamura-Enya, T., Phillips, D.H., 2007a. Mutagenicity and DNA adduct formation by the urban air pollutant 2-nitrobenzanthrone. Toxicol. Sci. 98, 445-457.

Arlt, V. M., Stiborova, M., Brocke, J. V., Simoes, M. L., Lord, G. M., Nortier, J. L., Hollstein, M., Phillips, D. H., and Schmeiser, H. H. (2007b). Aristolochic acid mutagenesis: molecular clues to the aetiology of Balkan endemic nephropathy-associated urothelial cancer. Carcinogenesis 28, 2253-2261.

Atencio, I.A., Ramachandra, M., Shabram, P., Demers, G.W., 2000. Calpain inhibitor 1 activates p53-dependent apoptosis in tumor cell lines. Cell Growth. Differ. 11, 247-253.

Balachandran, P., Wei, F., Lin, R.C., Khan, I.A., Pasco, D.S., 2005. Structure activity relationships of aristolochic acid analogues: toxicity in cultured renal epithelial cells. Kid. Inter. 67, 1797-1805.

Baron, V., Adamson, E.D., Calogero, A., Ragona, G., Mercola, D., 2006. The transcription factor Egr1 is a direct regulator of multiple tumor suppressors including TGFbeta1, PTEN, p53, and fibronectin. Cancer Gene Ther. 13, 115-124.

Bieler, C.A., Stiborova, M., Wiessler, M., Cosyns, J.P., van Ypersele de Strihou, C., Schmeiser, H.H., 1997. 32P-post-labelling analysis of DNA adducts formed by aristolochic acid in tissues from patients with Chinese herbs nephropathy. Carcinogenesis 18, 1063-1067.

Boiteux, S., Gajewski, E., Laval, J., Dizdaroglu, M., 1992. Substrate specificity of the Escherichia coli Fpg protein (formamidopyrimidine-DNA glycosylase): excision of purine lesions in DNA produced by ionizing radiation or photosensitization. Biochemistry 31, 106-110.

Bratt, T., 2000. Lipocalins and cancer. Biochim. Biophys. Acta. 1482, 318-326.

Broschard, T.H., Wiessler, M., von der Lieth, C.W., Schmeiser, H.H., 1994. Translesional synthesis on DNA templates containing site-specifically placed deoxyadenosine and deoxyguanosine adducts formed by the plant carcinogen aristolochic acid. Carcinogenesis 15, 2331-2340.

Bunz, F., Dutriaux, A., Lengauer, C., Waldman, T., Zhou, S., Brown, J.P., Sedivy, J.M., Kinzler, K. W., Vogelstein, B., 1998. Requirement for p53 and p21 to sustain G2 arrest after DNA damage. Science 282, 1497-1501.

Carver, L.A., Schnitzer, J.E., 2003. Caveolae: mining little caves for new cancer targets. Nature Rev. 3, 571-581.

Chang, H.R., Lian, J.D., Lo, C.W., Huang, H.P., Wang, C.J., 2007. Aristolochic acid-induced cell cycle G1 arrest in human urothelium SV-HUC-1 cells. Food Chem. Toxicol. 45, 396-402.

Chatterjee, A., Mambo, E., Osada, M., Upadhyay, S., Sidransky, D., 2006. The effect of p53-RNAi and p53 knockout on human 8-oxoguanine DNA glycosylase (hOgg1) activity. Faseb J. 20, 112-114.

Chen, T., Guo, L., Zhang, L., Shi, L., Fang, H., Sun, Y., Fuscoe, J.C., Mei, N., 2006. Gene expression profiles distinguish the carcinogenic effects of aristolochic acid in target (kidney) and non-target (liver) tissues in rats. BMC Bioinformatics 7 (Suppl 2), S20.

Christensen, E.I., Devuyst, O., Dom, G., Nielsen, R., Van der Smissen, P., Verroust, P., Leruth, M., Guggino, W.B., Courtoy, P.J., 2003. Loss of chloride channel ClC-5 impairs endocytosis by defective trafficking of megalin and cubilin in kidney proximal tubules. Proc. Natl. Acad. Sci. U S A 100, 8472-8477.

Cosyns, J.P., 2003. Aristolochic acid and 'Chinese herbs nephropathy': a review of the evidence to date. Drug Saf. 26, 33-48.

Cosyns, J.P., Jadoul, M., Squifflet, J.P., Wese, F.X., van Ypersele de Strihou, C., 1999. Urothelial lesions in Chinese-herb nephropathy. Am. J. Kidney Dis. 33, 1011-1017.

Del Bello, B., Moretti, D., Gamberucci, A., Maellaro, E., 2007. Cross-talk between calpain and caspase-3/-7 in cisplatin-induced apoptosis of melanoma cells: a major role of calpain inhibition in cell death protection and p53 status. Oncogene 26, 2717-2726.

Dennis, G., Jr., Sherman, B.T., Hosack, D.A., Yang, J., Gao, W., Lane, H.C., Lempicki, R.A., 2003. DAVID: Database for Annotation, Visualization, and Integrated Discovery. Genome Biol. 4, P3.

Dipple, A., Khan, Q.A., Page, J.E., Ponten, I., Szeliga, J., 1999. DNA reactions, mutagenic action and stealth properties of polycyclic aromatic hydrocarbon carcinogens (review). Int. J. Oncol. 14, 103-111.

Dornetshuber, R., Heffeter, P., Kamyar, M. R., Peterbauer, T., Berger, W., Lemmens-Gruber, R., 2007. Enniatin exerts p53-dependent cytostatic and p53-independent cytotoxic activities against human cancer cells. Chem. Res. Toxicol. 20, 465-473.

el-Deiry, W.S., Harper, J.W., O'Connor, P.M., Velculescu, V.E., Canman, C.E., Jackman, J., Pietenpol, J.A., Burrell, M., Hill, D.E., Wang, Y., et al., 1994. WAF1/CIP1 is induced in p53-mediated G1 arrest and apoptosis. Cancer Res. 54, 1169-1174.

Feldmeyer, N., Schmeiser, H.H., Muehlbauer, K.R., Belharazem, D., Knyazev, Y., Nedelko, T., Hollstein, M., 2006. Further studies with a cell immortalization assay to investigate the mutation signature of aristolochic acid in human p53 sequences. Mutat. Res. 608, 163-168.

Gauger, M.A., Sancar, A., 2005. Cryptochrome, circadian cycle, cell cycle checkpoints, and cancer. Cancer Res. 65, 6828-6834.

Gold, L.S., Slone, T.H., 2003. Aristolochic acid, an herbal carcinogen, sold on the Web after FDA alert. New Engl. J. Med. 349, 1576-1577.

Grimm, M.O., Jurgens, B., Schulz, W.A., Decken, K., Makri, D., Schmitz-Drager, B.J., 1995. Inactivation of tumor suppressor genes and deregulation of the c-myc gene in urothelial cancer cell lines. Urol. Res. 23, 293-300.

Grollman, A.P., Shibutani, S., Moriya, M., Miller, F., Wu, L., Moll, U., Suzuki, N., Fernandes, A., Rosenquist, T., Medverec, Z., Jakovina, K., Brdar, B., Slade, N., Turesky, R.J., Goodenough, A.K., Rieger, R., Vukelic, M., Jelakovic, B., 2007. Aristolochic acid and the etiology of endemic (Balkan) nephropathy. Proc. Natl. Acad. Sci. U S A 104, 12129-12134.

Guo, L., Lobenhofer, E.K., Wang, C., Shippy, R., Harris, S.C., Zhang, L., Mei, N., Chen, T., Herman, D., Goodsaid, F.M., Hurban, P., Phillips, K.L., Xu, J., Deng, X., Sun, Y.A., Tong, W., Dragan, Y.P., Shi, L., 2006. Rat toxicogenomic study reveals analytical consistency across microarray platforms. Nat. Biotech. 24, 1162-1169.

Habuchi, T., Kinoshita, H., Yamada, H., Kakehi, Y., Ogawa, O., Wu, W.J., Takahashi, R., Sugiyama, T., Yoshida, O., 1994. Oncogene amplification in urothelial cancers with p53 gene mutation or MDM2 amplification. J. Natl. Cancer Inst. 86, 1331-1335.

Hartwig, A., Dally, H., Schlepegrell, R., 1996. Sensitive analysis of oxidative DNA damage in mammalian cells: use of the bacterial Fpg protein in combination with alkaline unwinding. Toxicol. Lett. 88, 85-90.

Hockley, S.L., Arlt, V.M., Brewer, D., Giddings, I., Phillips, D.H., 2006. Time- and concentration-dependent changes in gene expression induced by benzo(a)pyrene in two human cell lines, MCF-7 and HepG2. BMC Genomics 7, 260.

Hockley, S.L., Arlt, V.M., Brewer, D., Te Poele, R., Workman, P., Giddings, I., Phillips, D.H., 2007. AHR- and DNA-Damage-Mediated Gene Expression Responses Induced by Benzo(a)pyrene in Human Cell Lines. Chem. Res Toxicol. 20, 1797-1810.

Hockley, S.L., Arlt, V.M., Jahnke, G., Hartwig, A., Giddings, I., Phillips, D.H., 2008. Identification through microarray gene expression analysis of cellular responses to benzo(a)pyrene and its diol-epoxide that are dependent or independent of p53. Carcinogenesis 29, 202-210.

Hosack, D.A., Dennis, G., Jr., Sherman, B.T., Lane, H.C., Lempicki, R.A., 2003. Identifying biological themes within lists of genes with EASE. Genome Biol. 4, R70.

Hsin, Y.H., Cheng, C.H., Tzen, J.T., Wu, M.J., Shu, K.H., Chen, H.C., 2006. Effect of aristolochic acid on intracellular calcium concentration and its links with apoptosis in renal tubular cells. Apoptosis 11, 2167-2177.

Hussain, S.P., Hollstein, M.H., Harris, C.C., 2000. p53 tumor suppressor gene: at the crossroads of molecular carcinogenesis, molecular epidemiology, and human risk assessment. Annals New York Acad. Sci. 919, 79-85.

Hvidberg, V., Jacobsen, C., Strong, R.K., Cowland, J.B., Moestrup, S.K., Borregaard, N., 2005. The endocytic receptor megalin binds the iron transporting neutrophil-gelatinase-associated lipocalin with high affinity and mediates its cellular uptake. FEBS Lett 579, 773-777.

IARC, 2002. Some tratitional herbal medicines, some mycotoxins, naphthalene and styrene. IARC Monogr. Eval. Carcinog. Risk. Hum. 82.

Kabanda, A., Jadoul, M., Lauwerys, R., Bernard, A., van Ypersele de Strihou, C., 1995. Low molecular weight proteinuria in Chinese herbs nephropathy. Kidney Int. 48, 1571-1576.

Kamai, T., Tsujii, T., Arai, K., Takagi, K., Asami, H., Ito, Y., Oshima, H., 2003. Significant association of Rho/ROCK pathway with invasion and metastasis of bladder cancer. Clin. Cancer Res. 9, 2632-2641.

Khan, Q. A., Vousden, K. H., Dipple, A., 1997. Cellular response to DNA damage from a potent carcinogen involves stabilization of p53 without induction of p21(waf1/cip1). Carcinogenesis 18, 2313-2318.

Khan, Q. A., Vousden, K.H., Dipple, A., 1999. Lack of p53-mediated G1 arrest in response to an environmental carcinogen. Oncology 57, 258-264.

Khan, Q. A., Dipple, A., 2000. Diverse chemical carcinogens fail to induce G(1) arrest in MCF-7 cells. Carcinogenesis 21, 1611-1618.

Krones-Herzig, A., Mittal, S., Yule, K., Liang, H., English, C., Urcis, R., Soni, T., Adamson, E.D., Mercola, D., 2005. Early growth response 1 acts as a tumor suppressor in vivo and in vitro via regulation of p53. Cancer Res. 65, 5133-5143.

Lanzetti, L., Di Fiore, P.P., Scita, G., 2001. Pathways linking endocytosis and actin cytoskeleton in mammalian cells. Exp. Cell Res. 271, 45-56.

Lebeau, C., Arlt, V.M., Schmeiser, H.H., Boom, A., Verroust, P.J., Devuyst, O., Beauwens, R., 2001. Aristolochic acid impedes endocytosis and induces DNA adducts in proximal tubule cells. Kidney Int. 60, 1332-1342.

Lebeau, C., Debelle, F.D., Arlt, V.M., Pozdzik, A., De Prez, E.G., Phillips, D.H., Deschodt-Lanckman, M.M., Vanherweghem, J.L., Nortier, J.L., 2005. Early proximal tubule injury in experimental aristolochic acid nephropathy: functional and histological studies. Nephrol. Dial. Transplant. 20, 2321-2332.

Lee, J.N., Ye, J., 2004. Proteolytic activation of sterol regulatory element-binding protein induced by cellular stress through depletion of Insig-1. J. Biol. Chem. 279, 45257-45265.

Li, Y., Liu, Z., Guo, X., Shu, J., Chen, Z., Li, L., 2006. Aristolochic acid I-induced DNA damage and cell cycle arrest in renal tubular epithelial cells in vitro. Arch. Toxicol. 80, 524-532.

Liu, Z., Hergenhahn, M., Schmeiser, H.H., Wogan, G.N., Hong, A., Hollstein, M., 2004. Human tumor p53 mutations are selected for in mouse embryonic fibroblasts harboring a humanized p53 gene. Proc. Natl. Acad. Sci. U S A 101, 2963-2968.

Lord, G.M., Cook, T., Arlt, V.M., Schmeiser, H.H., Williams, G., Pusey, C.D., 2001. Urothelial malignant disease and Chinese herbal nephropathy. Lancet 358, 1515-1516.

Lord, G.M., Hollstein, M., Arlt, V.M., Roufosse, C., Pusey, C.D., Cook, T., Schmeiser, H.H., 2004. DNA adducts and p53 mutations in a patient with aristolochic acid-associated nephropathy. Am. J. Kidney Dis. 43, e11-17.

McDermott, U., Longley, D.B., Galligan, L., Allen, W., Wilson, T., Johnston, P.G., 2005. Effect of p53 status and STAT1 on chemotherapy-induced, Fas-mediated apoptosis in colorectal cancer. Cancer Res. 65, 8951-8960.

Mei, N., Arlt, V.M., Phillips, D.H., Heflich, R.H., Chen, T., 2006. DNA adduct formation and mutation induction by aristolochic acid in rat kidney and liver. Mutat. Res. 602, 83-91.

Milde-Langosch, K. (2005). The Fos family of transcription factors and their role in tumourigenesis. Eur J Cancer 41, 2449-2461.

Neumar, R.W., Xu, Y.A., Gada, H., Guttmann, R.P., Siman, R., 2003. Cross-talk between calpain and caspase proteolytic systems during neuronal apoptosis. J. Biol. Chem. 278, 14162-14167.

Nilsson, J.A., Cleveland, J.L., 2003. Myc pathways provoking cell suicide and cancer. Oncogene 22, 9007-9021.

Nortier, J.L., Martinez, M.C., Schmeiser, H.H., Arlt, V.M., Bieler, C.A., Petein, M., Depierreux, M. F., De Pauw, L., Abramowicz, D., Vereerstraeten, P., Vanherweghem, J.L., 2000. Urothelial carcinoma associated with the use of a Chinese herb (Aristolochia fangchi). New Engl. J. Med. 342, 1686-1692.

Ohtsuka, T., Jensen, M.R., Kim, H.G., Kim, K.T., Lee, S.W., 2004. The negative role of cyclin G in ATM-dependent p53 activation. Oncogene 23, 5405-5408.

Okada, H., Watanabe, Y., Inoue, T., Kobayashi, T., Kanno, Y., Shiota, G., Nakamura, T., Sugaya, T., Fukamizu, A., Suzuki, H., 2003. Transgene-derived hepatocyte growth factor attenuates reactive renal fibrosis in aristolochic acid nephrotoxicity. Nephrol. Dial. Transplant. 18, 2515-2523.

Park, W.Y., Hwang, C.I., Im, C.N., Kang, M.J., Woo, J.H., Kim, J.H., Kim, Y.S., Kim, J.H., Kim, H., Kim, K.A., Yu, H.J., Lee, S.J., Lee, Y.S., Seo, J.S., 2002. Identification of radiation-specific responses from gene expression profile. Oncogene 21, 8521-8528.

Petitjean, A., Mathe, E., Kato, S., Ishioka, C., Tavtigian, S. V., Hainaut, P., Olivier, M., 2007. Impact of mutant p53 functional properties on TP53 mutation patterns and tumor phenotype: lessons from recent developments in the IARC TP53 database. Human Mutat. 28, 622-629.

Phillips, D.H., Arlt, V.M. (2007). The 32P-postlabeling assay for DNA adducts. Nat. Protoc. 2, 2772-2781.

Pineiro, D., Martin, M.E., Guerra, N., Salinas, M., Gonzalez, V.M., 2007. Calpain inhibition stimulates caspase-dependent apoptosis induced by taxol in NIH3T3 cells. Exp. Cell Res. 313, 369-379.

Pozdzik, A.A., Salmon, I.J., Debelle, F.D., Decaestecker, C., Van den Branden, C., Verbeelen, D., Deschodt-Lanckman, M.M., Vanherweghem, J.L., Nortier, J.L., 2008. Aristolochic acid induces proximal tubule apoptosis and epithelial to mesenchymal transformation. Kid. Int. 73, 595-607.

Preitner, N., Damiola, F., Lopez-Molina, L., Zakany, J., Duboule, D., Albrecht, U., Schibler, U., 2002. The orphan nuclear receptor REV-ERBalpha controls circadian transcription within the positive limb of the mammalian circadian oscillator. Cell 110, 251-260.

Qi, X., Cai, Y., Gong, L., Liu, L., Chen, F., Xiao, Y., Wu, X., Li, Y., Xue, X., Ren, J., 2007. Role of mitochondrial permeability transition in human renal tubular epithelial cell death induced by aristolochic acid. Toxicol. Appl. Pharmacol. 222, 105-110.

Ricordy, R., Gensabella, G., Cacci, E., Augusti-Tocco, G., 2002. Impairment of cell cycle progression by aflatoxin B1 in human cell lines. Mutagenesis 17, 241-249.

Ritter, B., Philie, J., Girard, M., Tung, E.C., Blondeau, F., McPherson, P.S., 2003. Identification of a family of endocytic proteins that define a new alpha-adaptin ear-binding motif. EMBO Rep. 4, 1089-1095.

Roos, W. P., Kaina, B., 2006. DNA damage-induced cell death by apoptosis. Trends Mol. Med. 12, 440-450.

Schmeiser, H.H., Janssen, J.W., Lyons, J., Scherf, H.R., Pfau, W., Buchmann, A., Bartram, C.R., Wiessler, M., 1990. Aristolochic acid activates ras genes in rat tumors at deoxyadenosine residues. Cancer Res. 50, 5464-5469.

Schmeiser, H.H., Bieler, C.A., Wiessler, M., van Ypersele de Strihou, C., Cosyns, J.P., 1996. Detection of DNA adducts formed by aristolochic acid in renal tissue from patients with Chinese herbs nephropathy. Cancer Res. 56, 2025-2028.

Schulz, W.A., 2006. Understanding urothelial carcinoma through cancer pathways. Int. J. Cancer 119, 1513-1518.

Schulz, W.A., Jankevicius, F., Gerharz, C.D., Kushima, M., van Roeyen, C., Bultel, H., Gobell, P., Schmitz-Drager, B.J., 1998. Predictive value of molecular alterations for the prognosis of urothelial carcinoma. Cancer Detect. Prev. 22, 422-429.

Schwerdtle, T., Walter, I., Mackiw, I., Hartwig, A., 2003. Induction of oxidative DNA damage by arsenite and its trivalent and pentavalent methylated metabolites in cultured human cells and isolated DNA. Carcinogenesis 24, 967-974.

Staib, F., Robles, A.I., Varticovski, L., Wang, X.W., Zeeberg, B.R., Sirotin, M., Zhurkin, V.B., Hofseth, L.J., Hussain, S.P., Weinstein, J.N., Galle, P.R., Harris, C.C., 2005. The p53 tumor suppressor network is a key responder to microenvironmental components of chronic inflammatory stress. Cancer Res. 65, 10255-10264.

Stein, G.S., van Wijnen, A.J., Stein, J.L., Lian, J.B., Montecino, M., Zaidi, S.K., Braastad, C., 2006. An architectural perspective of cell-cycle control at the G1/S phase cell-cycle transition. J. Cell. Phys. 209, 706-710.

Stemmer, K., Ellinger-Ziegelbauer, H., Ahr, H.J., Dietrich, D.R., 2007. Carcinogen specific gene expression profiles in short-term treated Eker and wild type rats indicative for pathways involved in renal tumourigenesis. Cancer Res. 67, 4052-4068.

Stiborova, M., Fernando, R.C., Schmeiser, H.H., Frei, E., Pfau, W., Wiessler, M., 1994. Characterization of DNA adducts formed by aristolochic acids in the target organ (forestomach) of rats by 32P-postlabelling analysis using different chromatographic procedures. Carcinogenesis 15, 1187-1192.

Stiborova, M., Frei, E., Hodek, P., Wiessler, M., Schmeiser, H.H., 2005. Human hepatic and renal microsomes, cytochromes P450 1A1/2, NADPH:cytochrome P450 reductase and

prostaglandin H synthase mediate the formation of aristolochic acid-DNA adducts found in patients with urothelial cancer. Int. J. Cancer 113, 189-197.

Stiborova, M., Frei, E., Arlt, V.M., Schmeiser, H.H., 2008. Metabolic activation of carcinogenic aristolochic acid, a risk factor for Balkan endemic nephropathy. Mutat. Res. 658, 55-67.

Tchou, J., Kasai, H., Shibutani, S., Chung, M.H., Laval, J., Grollman, A.P., Nishimura, S., 1991. 8-oxoguanine (8-hydroxyguanine) DNA glycosylase and its substrate specificity. Proc. Natl. Acad. Sci.U S A 88, 4690-4694.

Vanherweghem, J.L., Depierreux, M., Tielemans, C., Abramowicz, D., Dratwa, M., Jadoul, M., Richard, C., Vandervelde, D., Verbeelen, D., Vanhaelen-Fastre, R., and et al., 1993. Rapidly progressive interstitial renal fibrosis in young women: association with slimming regimen including Chinese herbs. Lancet 341, 387-391.

Vikhanskaya, F., Lee, M.K., Mazzoletti, M., Broggini, M., Sabapathy, K., 2007. Cancer-derived p53 mutants suppress p53-target gene expression--potential mechanism for gain of function of mutant p53. Nucleic acids research.

vom Brocke, J., Schmeiser, H.H., Reinbold, M., Hollstein, M., 2006. MEF immortalization to investigate the ins and outs of mutagenesis. Carcinogenesis 27, 2141-2147.

Wheeler, A.P., Ridley, A.J., 2004. Why three Rho proteins? RhoA, RhoB, RhoC, and cell motility. Exp. Cell Res. 301, 43-49.

Williams, T.M., Lisanti, M.P., 2005. Caveolin-1 in oncogenic transformation, cancer, and metastasis. Am. J. Physiol. 288, C494-506.

Wu, K.M., Farrelly, J.G., Upton, R., Chen, J., 2007. Complexities of the herbal nomenclature system in traditional Chinese medicine (TCM): Lessons learned from the misuse of Aristolochia-related species and the importance of the pharmaceutical name during botanical drug product development. Phytomedicine 14, 273-279.

Table 1

Genes with expression significantly different (*P*<0.05; 1-Way ANOVA) between HCT116 p53-WT and p53-null cells after exposure to 100 μM AAI for 24 and 48 hours

				24 h		48 h	
Image Clone ID[a]	**Gene symbol**	**Genbank ID**	**Description**	**p53-WT**	**p53-null**	**p53-WT**	**p53-null**
207288	*INSIG1*	NM_198336	Insulin induced gene 1	0.79	0.89	0.58	0.94
358457	*HNRPH1*	BX647205	Heterogeneous nuclear ribonucleoprotein H1 (H)	1.20	1.04	1.60	1.10
810504	*PLP2*	BF214130	Proteolipid protein 2 (colonic epithelium-enriched)	0.66	0.78	0.63	0.71
840944	*EGR1*	NM_001964	Early growth response 1	3.14	2.33	3.25	2.02
269745	*DCBLD2*	NM_080927	Discoidin, CUB and LCCL domain containing 2	0.91	0.80	0.86	0.64
32134	*DNAJC9*	AK094162	DnaJ (Hsp40) homolog, subfamily C, member 9	0.69	0.82	0.73	0.83
377461	*CAV1*	NM_001753	Caveolin 1, caveolae protein, 22kDa	0.86	0.80	0.93	0.70
795330	*NR1D1*	M24898	Nuclear receptor subfamily 1, group D, member 1	1.31	1.87	1.84	2.58
741497	*LCN2*	BU174414	Lipocalin 2 (oncogene 24p3)	0.65	0.94	0.54	0.94
32834	*SQLE*	BX647605	Squalene epoxidase	0.62	0.87	0.70	0.82
200862	*CAV1*	NM_001753	Caveolin 1, caveolae protein, 22kDa	0.87	0.73	0.88	0.66
269119	*CAV1*	NM_001753	Caveolin 1, caveolae protein, 22kDa	0.83	0.70	0.84	0.70
814798	*ALDH1A3*	AF198444	Aldehyde dehydrogenase 1 family, member A3	1.56	1.15	1.59	0.97
205819	*CPM*	NM_001874	Carboxypeptidase M	1.32	1.01	1.83	0.97
1711438	*MIF*	BQ056329	Macrophage migration inhibitory factor (glycosylation-inhibiting factor)	1.07	0.76	0.95	0.70
35516	*CCNG1*	NM_004060	Cyclin G1	0.88	0.70	0.87	0.61
253009	*MALAT1*	BX538238	Metastasis associated lung adenocarcinoma transcript 1 (non-coding RNA)	0.62	1.01	0.68	0.95
41979	*FLJ14525*	BC066649	Hypothetical protein FLJ14525	0.65	0.94	0.63	0.85

[a] Image clone 150085 has been significantly (*P*<0.05) modulated but no gene symbol and/or Genbank ID was identified.

Table 2

Biological processes significantly over-represented (EASE Score<0.05) within the gene expression profiles induced after exposure to 100 μM AAI for 24 and 48 hours in HCT116 p53-WT and p53-null cells

Biological Process	p53-WT	p53-null
RNA splicing; RNA processing; RNA metabolism	PPP2CA; RNPC2; SF3A1; SFPQ; SFRS1; SFRS10; SFRS3; SFRS7; CSTF3; HNRPH1 ↑[a]	CSTF3; HNRPDL; RNPC2; SF3A1; SFPQ; SFRS1; SFRS10; SFRS7; YARS ↑
mRNA splicing; mRNA processing; mRNA metabolism	CSTF3; RNPC2; SF3A1; SFPQ; SFRS1; SFRS10; SFRS3; SFRS7 ↑	CSTF3; RNPC2; SF3A1; SFPQ; SFRS1; SFRS10; SFRS7 ↑
metabolism	AGA; ALDH1A3; ATF3; CHD2; CPM; CSE1L; CSTF3; EGR1; IF2S1;EIF2S2; FHL2; FLJ10378; FLJ11021; GOT1; HIST1H2AC; HNRPH1; NFKBIA; NR1D1; NR1D2; ODC1; PIP5K1A; PPP2CA; PPP2R2A; PTP4A1; RNPC2; SF3A1; SFPQ; SFRS1; SFRS10; SFRS3; SFRS7;TCERG1; TOMM34; UBE2V2; XRCC4; ZYX ↑	ARSF; ATF3; CHD2; CSTF3; EGR1; FLJ10378; FLJ11021; GOT1; HIST1H1C; HIST1H2AC; HIST1H3D; HNRPDL; MYC; NR1D1; NR1D2; NTRK2; ODC1; PPP2R2A; PTP4A1; RNPC2; RPA2; SF3A1; SFPQ; SFRS1; SFRS10; SFRS7; SLC3A2; TOMM34; YARS ↑
nucleobase, nucleoside, nucleotide and nucleic acid metabolism	ATF3; CHD2; CSTF3; EGR1; FHL2; FLJ11021; HIST1H2AC; HNRPH1; NR1D1; NR1D2; PPP2CA; RNPC2; SF3A1; SFPQ; SFRS1; SFRS10; SFRS3; SFRS7; TCERG1; UBE2V2; XRCC4 ↑	ATF3; CHD2; CSTF3; EGR1; FLJ11021; HIST1H1C; HIST1H2AC; HIST1H3D; HNRPDL; MYC; NR1D1; NR1D2; RNPC2; RPA2; SF3A1; SFPQ; SFRS1; SFRS10; SFRS7; YARS ↑
chromatin assembly/disassembly	CHD2; FLJ11021; HIST1H2AC ↑	CHD2; FLJ11021; HIST1H1C; HIST1H2AC; HIST1H3D ↑
nucleosome assembly	–[b]	FLJ11021; HIST1H1C; HIST1H2AC; HIST1H3D ↑
chromatin architecture; chromosome organization	–	CHD2; FLJ11021; HIST1H1C; HIST1H2AC; HIST1H3D ↑
DNA packaging	–	CHD2; FLJ11021; HIST1H1C; HIST1H2AC; HIST1H3D ↑
physiological process	–	AP3S1; ARSF; ATF3; CHD2; CSTF3; EGR1; FLJ10378; FLJ11021; GOT1; HIST1H1C; HIST1H2AC; HIST1H3D; HNRPDL; MT1F; MYC; NR1D1; NR1D2; NTRK2; ODC1; PPP2R2A; PTP4A1; RNPC2; RPA2; SF3A1; SFPQ; SFRS1; SFRS10; SFRS7; SLC3A2; TOMM34; YARS ↑
DNA metabolism	–	CHD2; FLJ11021; HIST1H1C; HIST1H2AC; HIST1H3D; RPA2 ↑
protein biosynthesis	–	DDOST; IARS; RPL10; RPL12; RPL21; RPL27A; RPL31; RPL37A; RPS16; RPS9 ↓[a]
macromolecule biosynthesis	–	DDOST; FDFT1; IARS; RPL10; RPL12; RPL21; RPL27A; RPL31; RPL37A; RPS16; RPS9; SCD ↓
biosynthesis	–	DDOST; FDFT1; IARS; RPL10; RPL12; RPL21; RPL27A; RPL31; RPL37A;

		RPS16; RPS9; SCD ↓
ribosome biogenesis and assembly	–	RPL12; RPL21; RPS16 ↓
protein folding	–	DNAJB11; HSPA8; PPIB; TRA1 ↓
protein metabolism	–	DDOST; DNAJB11; HSPA8; IARS; PLAT; PPIB; RPL10; RPL12; RPL21; RPL27A; RPL31; RPL37A; RPS16; RPS9; TRA1; UBE2M ↓
secretion	–	CANX; ERP70; SYN2 ↓

[a] ↑ up-regulated expression; ↓ down-regulated expression.

[b] –, no over-represented gene expression alterations were found.

Table 3

Differential expression of selected genes in HCT116 p53-WT and p53-null cells after exposure to 100 μM AAI for 48 h

	p53-WT			p53-null		
Gene	RT-PCR[a] [fold-change]	RT-PCR [direction]	Microarray [direction]	RT-PCR [fold-change]	RT-PCR [direction]	Microarray [direction]
ALDH1A3	3.0	↑	↑	1.0	–	–
CCNG1	1.8	↑	–	0.2	↓	↓
HIST1H4B	5.3	↑	↑	1.3	–	↑
SCD	0.1	↓	↓	0.2	↓	↓
MYC	6.4	↑	–	2.6	↑	↑
FOS	0.1	↓	↓	0.1	↓	↓
ROHB	2.2	↑	–	2.7	↑	↑
NR1D1	63.8	↑	↑	22.3	↑	↑
CAV1	0.99	–	–	0.5	↓	↓
CDKN1A	18.6	↑	↑	1.3	–	–
CYP1A1	6.6	↑	⊗	2.4	↑	⊗

[a] All results represent mean of three incubations; each sample was determined by three separate analyses. ↑ = up-regulated; ↓ = down-regulated; – = unaltered expression; ⊗ = gene not present on microarray.

Legend to Figures:

Figure 1

Effect of AAI on viability (% control) of (A) HCT116 p53-WT and (B) HCT116 p53-null cells. Values represent means of two independent experiments.

Figure 2

Quantitative ^{32}P-postlabelling analysis of total AA-DNA adducts in (A) HCT116 p53-WT and (B) HCT116 p53-null cells. Insets: autoradiographic profile of AA-DNA adducts obtained in (A) HCT116 p53-WT and (B) HCT116 p53-null cells after exposure to 100 μM AAI for 48 h. The origin, in the bottom left-hand corner, was cut off before exposure. Spot 1, dA-AAI; spot 2, dG-AAI; spot 3, dA-AAII. 3-NBA (5 μM) was used as a positive control (Hockley *et al.*, 2008).

Figure 3

Venn diagram illustrating the overlap of gene expression profiles of HCT116 p53-WT and HCT116 p53-null cells induced by AAI exposure altered by at least 1.4-fold (P<0.05). Gene expression changes after exposure to (A) 50 or 100 μM AAI for 6, 24 or 48 h and (B) 100 μM AAI for 24 or 48 h.

Figure 4

Gene expression analysis of HCT116 cells exposed to AAI. (A) Hierarchical clustering and (B) Principal component analysis of genes modulated in at least one of the cell lines after AAI exposure to 50 or 100 μM AAI for 6, 24 or 48 h (210 genes).

Figure 5

Western blot analysis of (A) TP53 and (B) CDKN1A protein expression in HCT116 cells exposed to AAI. GAPDH antibody was used to detect GAPDH protein expression, which was used as loading control.

Figure 6

Apoptosis assay in (A) HCT116 p53-WT and (B) HCT116 p53-null exposed to 100 μM AAI. The activities of caspase-3 and caspase-7 were measured by luminescence detection. The values are the mean ± SD (n=6). 3-NBA (5 μM) was used as a positive control.

Figure 7

Cell cycle parameters in (A) HCT116 p53-WT and (B) HCT116 p53-null exposed to 100 μM AAI. The values are the mean ± SD of six determinations (triplicate analyses of two separate cell incubations).

Figure 8

Induction of DNA strand breaks and oxidative DNA base modifications in (A) HCT116 p53-WT and (B) HCT116 p53-null exposed to 100 μM AAI. The frequencies of DNA strand breaks and Fpg-sensitive sites were determined by alkaline unwinding as described in the Material and Methods. The values are the mean ± SD of six determinations (triplicate analyses of two separate cell incubations). Shown are induced lesions; background levels of Fpg-sensitive sites in untreated p53-WT and p53-null cells were 0.035 ± 0.025 and 0.034 ± 0.021 per 10^6 base pairs, respectively. Hydrogen peroxide (H_2O_2; 100 μM; 5 min on ice) was used as a positive control.

Figure 9

Postulated mechanistic pathways of AA-induced toxicity (adapted and modified from (Stemmer *et al.*, 2007)). Black, pathways and processes suggested from the literature; blue, pathways and processes implicated by gene expression analysis; green, pathways and processes determined by biological analysis and corroborated by gene expression analysis. ER, endoplasmic reticulum. ?, unknown pathway in response to AA exposure.

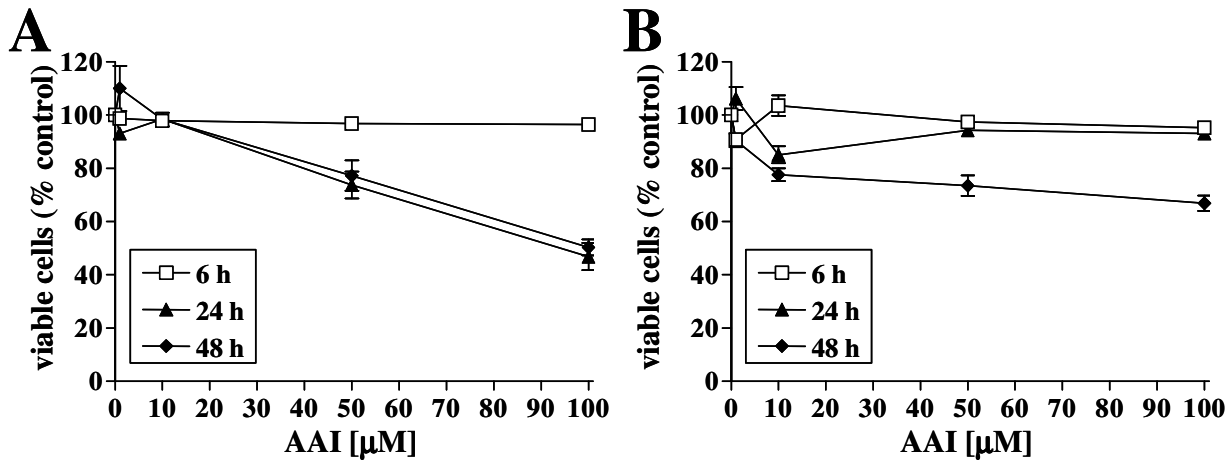
A
B
viable cells (% control)
AAI [µM]
6 h
24 h
48 h
0
20
40
60
80
100
120
0 10 20 30 40 50 60 70 80 90 100

Figure 1

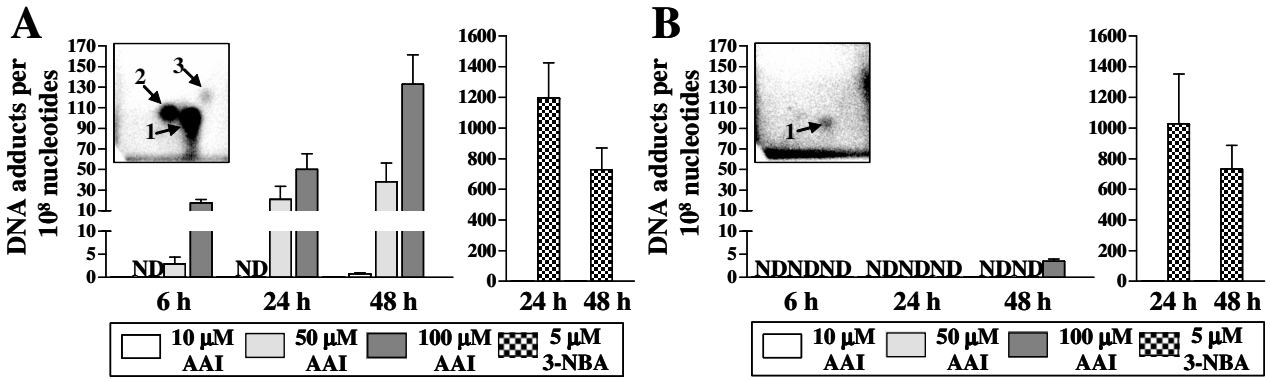
A
B
DNA adducts per 10⁸ nucleotides
1
2
3
ND
6 h
24 h
48 h
10 µM AAI
50 µM AAI
100 µM AAI
5 µM 3-NBA

Figure 2

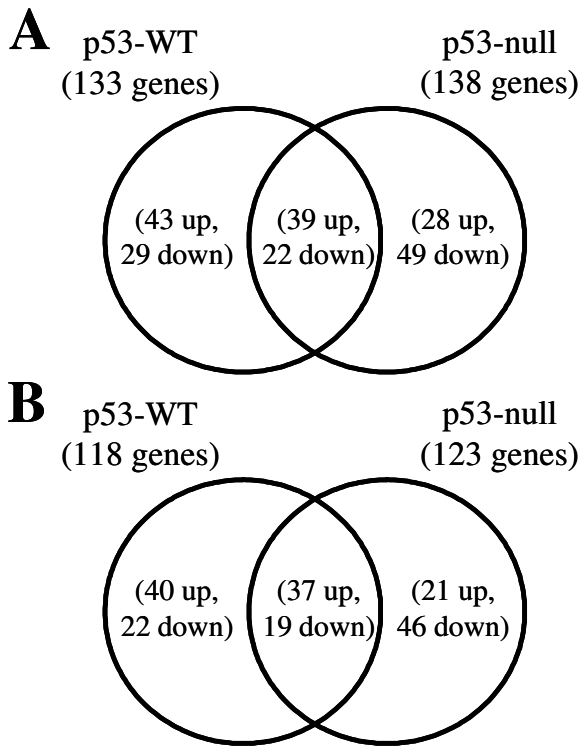
A
p53-WT
(133 genes)
p53-null
(138 genes)
(43 up,
29 down)
(39 up,
22 down)
(28 up,
49 down)
B
p53-WT
(118 genes)
p53-null
(123 genes)
(40 up,
22 down)
(37 up,
19 down)
(21 up,
46 down)

Figure 3

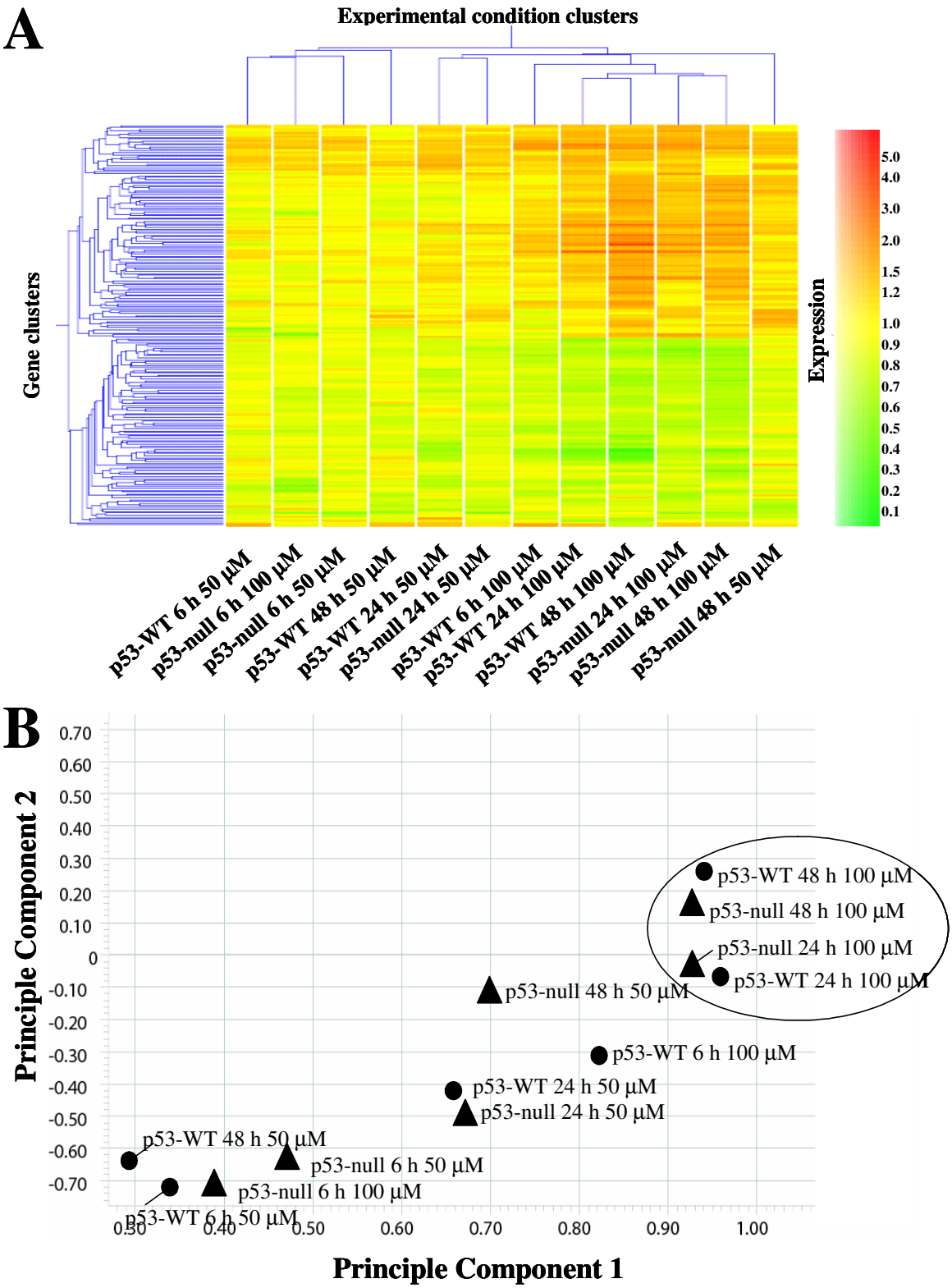
A
Experimental condition clusters
Gene clusters
Expression
5.0
4.0
3.0
2.0
1.5
1.2
1.0
0.9
0.8
0.7
0.6
0.5
0.4
0.3
0.2
0.1
p53-WT 6 h 50 µM
p53-null 6 h 100 µM
p53-null 6 h 50 µM
p53-WT 48 h 50 µM
p53-WT 24 h 50 µM
p53-null 24 h 50 µM
p53-WT 6 h 100 µM
p53-WT 24 h 100 µM
p53-WT 48 h 100 µM
p53-null 24 h 100 µM
p53-null 48 h 100 µM
p53-null 48 h 50 µM
B
Principle Component 2
0.70
0.60
0.50
0.40
0.30
0.20
0.10
0
-0.10
-0.20
-0.30
-0.40
-0.50
-0.60
-0.70
p53-WT 48 h 100 µM
p53-null 48 h 100 µM
p53-null 24 h 100 µM
p53-WT 24 h 100 µM
p53-null 48 h 50 µM
p53-WT 6 h 100 µM
p53-WT 24 h 50 µM
p53-null 24 h 50 µM
p53-WT 48 h 50 µM
p53-null 6 h 50 µM
p53-null 6 h 100 µM
p53-WT 6 h 50 µM
0.30
0.40
0.50
0.60
0.70
0.80
0.90
1.00
Principle Component 1

Figure 4

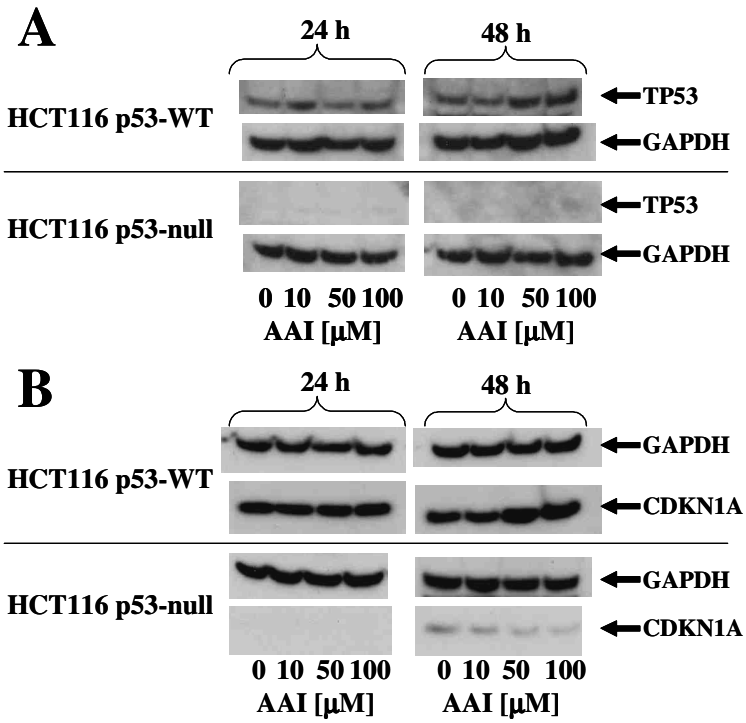
A
24 h
48 h
HCT116 p53-WT
TP53
GAPDH
HCT116 p53-null
TP53
GAPDH
0 10 50 100
AAI [μM]
0 10 50 100
AAI [μM]
B
24 h
48 h
HCT116 p53-WT
GAPDH
CDKN1A
HCT116 p53-null
GAPDH
CDKN1A
0 10 50 100
AAI [μM]
0 10 50 100
AAI [μM]

Figure 5

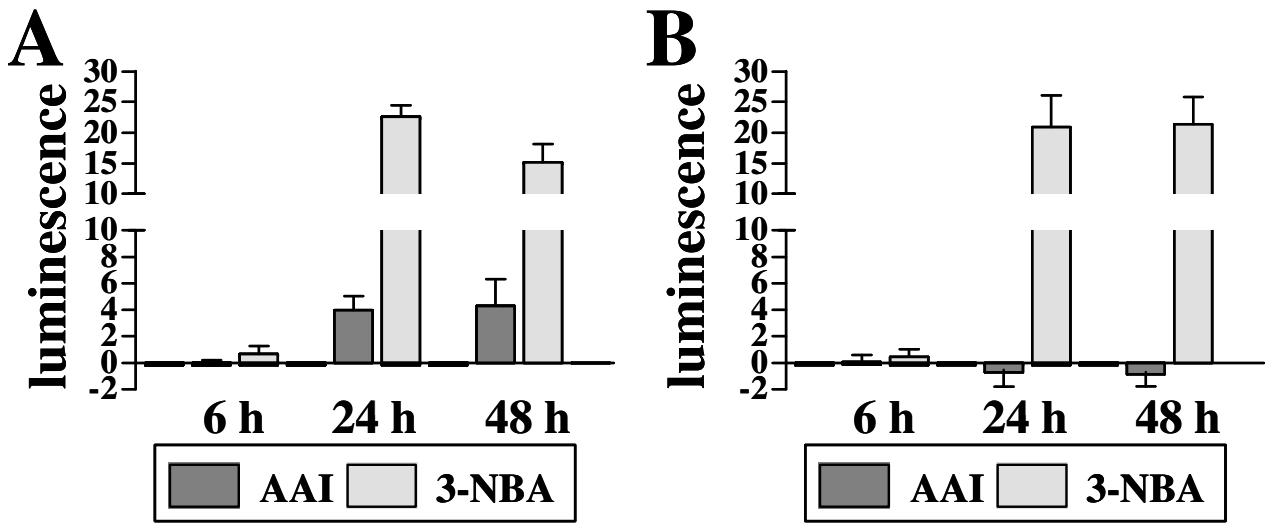
A
luminescence
30
25
20
15
10
10
8
6
4
2
0
-2
6 h
24 h
48 h
AAI
3-NBA
B
luminescence
30
25
20
15
10
10
8
6
4
2
0
-2
6 h
24 h
48 h
AAI
3-NBA

Figure 6

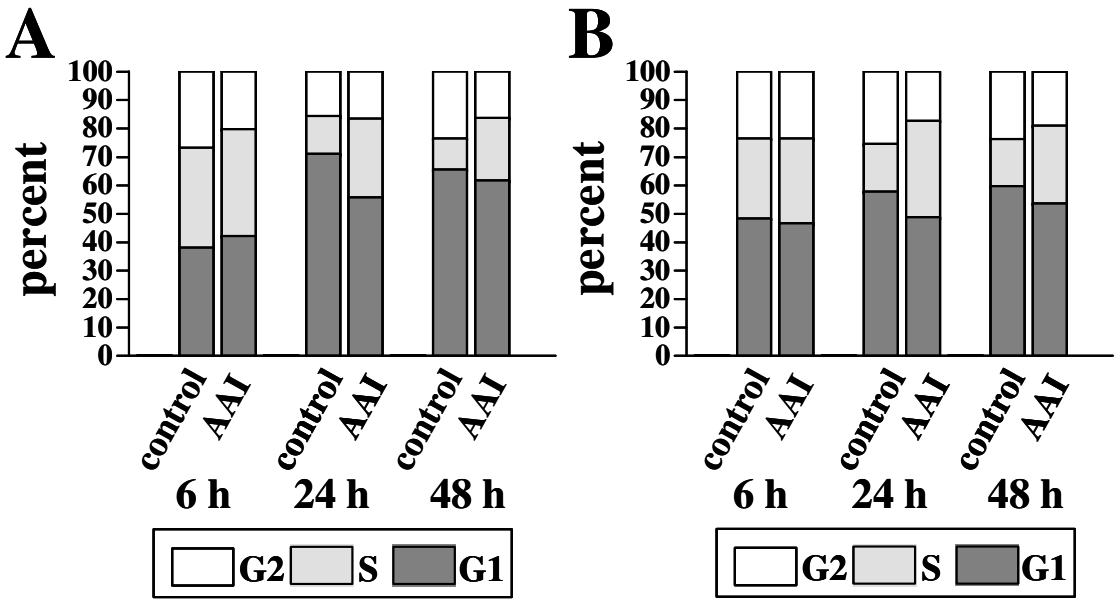
A
B
percent
100
90
80
70
60
50
40
30
20
10
0
control
AAI
6 h
24 h
48 h
G2
S
G1

Figure 7

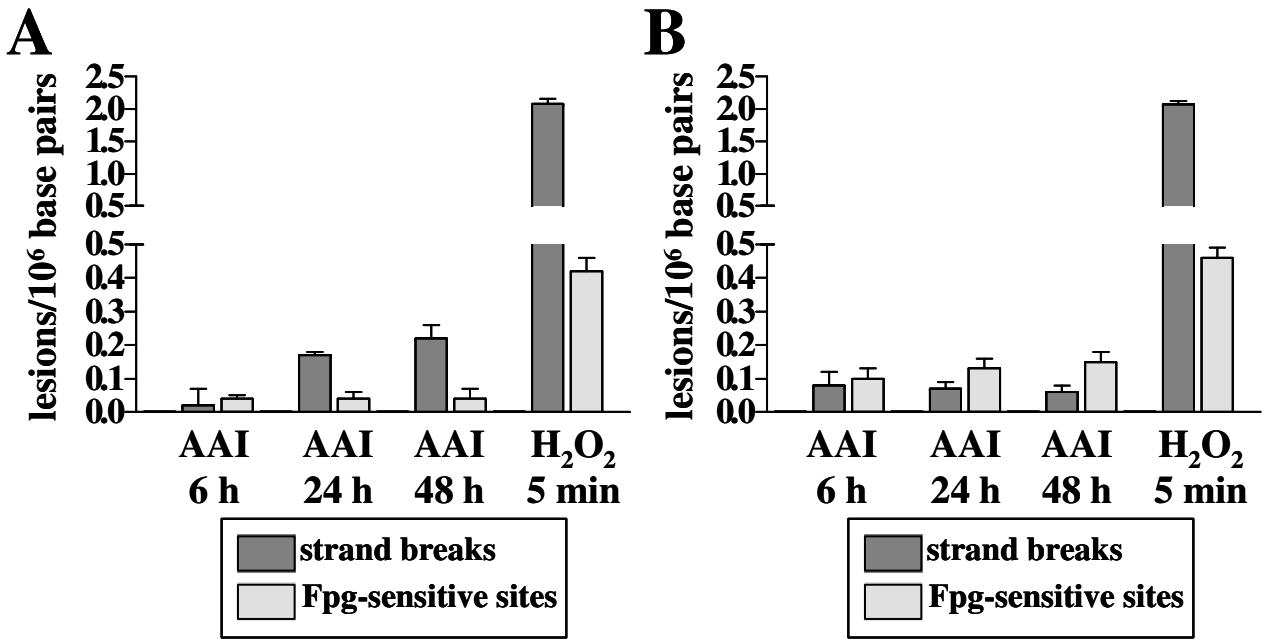
A
B
lesions/10⁶ base pairs
2.5
2.0
1.5
1.0
0.5
0.5
0.4
0.3
0.2
0.1
0.0
AAI 6 h
AAI 24 h
AAI 48 h
H2O2 5 min
strand breaks
Fpg-sensitive sites

Figure 8

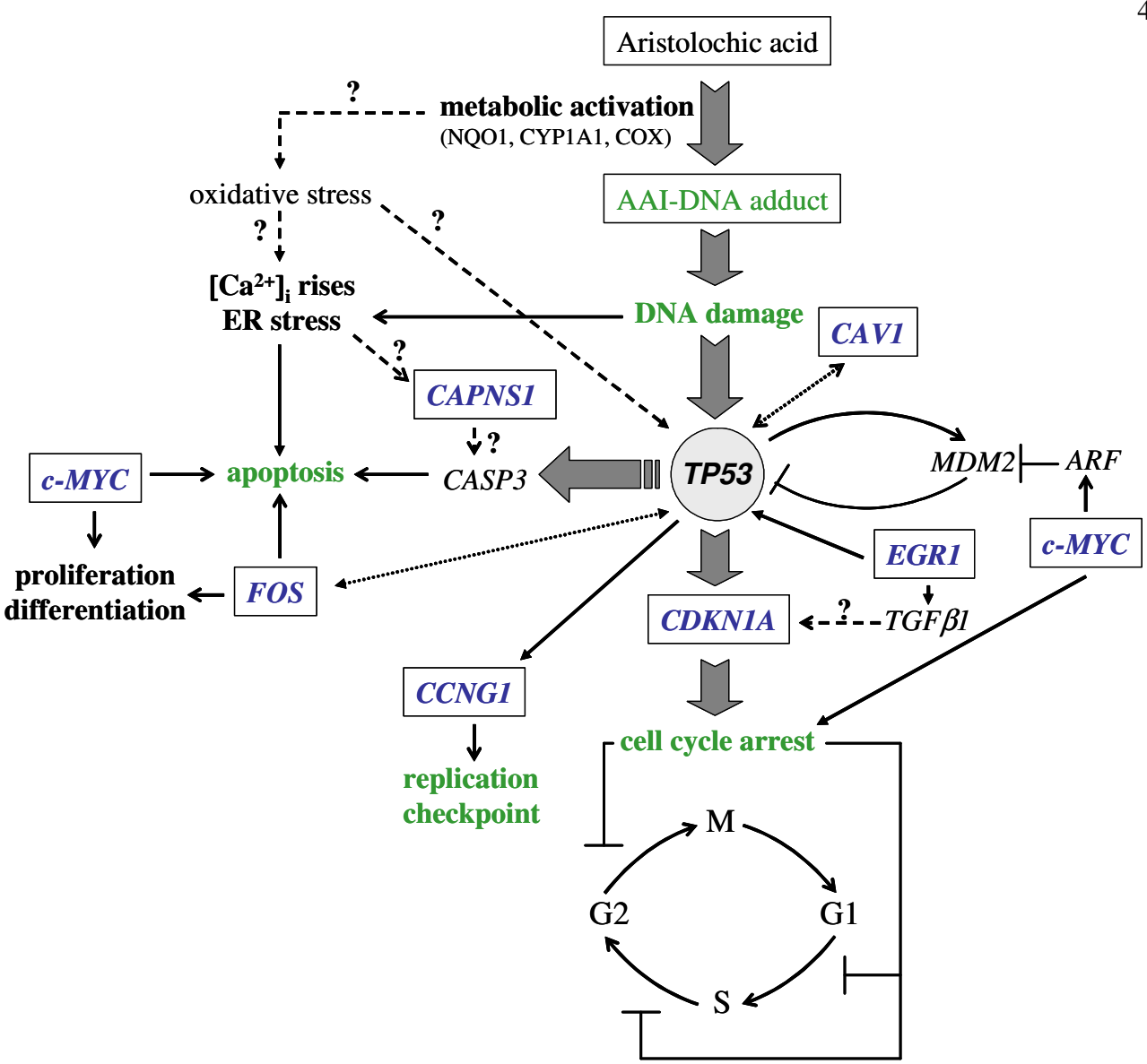
Aristolochic acid
metabolic activation
(NQO1, CYP1A1, COX)
AAI-DNA adduct
DNA damage
CAV1
oxidative stress
[Ca2+]i rises
ER stress
CAPNS1
c-MYC
apoptosis
CASP3
TP53
MDM2
ARF
c-MYC
EGR1
proliferation
differentiation
FOS
CDKN1A
TGFβ1
CCNG1
cell cycle arrest
replication
checkpoint
M
G2
G1
S

Figure 9